University of Pretoria

Tyre Inflation Pressure control to improve vehicle ride comfort on rough roads

by

Tokologo M.G. Komana

Submitted in partial fulfilment of the requirements for the degree

Masters in Engineering (Mechanical Engineering)

in the

FACULTY OF ENGINEERING, THE BUILT ENVIRONMENT AND INFORMATION TECHNOLOGY (EBIT)

UNIVERSITY OF PRETORIA

Pretoria

2020

It is hereby declared that this is my own work and appropriate reference has been made to other people's work.

© University of Pretoria

This page is intentionally left blank

© University of Pretoria

Abstract

Title: Tyre Inflation Pressure control to improve vehicle ride comfort on rough roads

Author: Tokologo M.G. Komana

Supervisor: Prof. P.S. Els

Department: Mechanical and Aeronautical Engineering, University of Pretoria

Degree: Masters in Engineering (Mechanical Engineering**)**

Tyres behave similar to a spring and damper systems smoothing out road irregularities as the tyre rolls. Tyre stiffness and damping characteristics are largely influenced by the tyre pressure. As a result, tyre pressure has an influence on tyre enveloping and ride comfort.

To take advantage of the influence of tyre pressure on ride comfort, a pressure controlled tyre was developed to vary the tyre pressure, thus varying the tyre characteristics as the road conditions change to improve ride comfort. Literature exists on TIS (Tyre Inflation Systems) and smart suspension control strategies optimised for ride comfort, which indicate that a pressure controlled tyre can be developed by managing a TIS with a ride comfort controller.

A VDG (Vehicle Dynamics Group) test trailer was used to complete this study. The trailer was modelled on three platforms; MATLAB, Cosin and ADAMS View; with the co-simulation managed through Simulink. Three tests were conducted to parametrise and validate the model, namely; pneumatic system parametrisation tests, APG (Aberdeen Proving Ground) bump tests and Belgian paving tests. The pneumatic system parametrisation tests show that the discharge coefficient is approximately 0.07 for choked flow and tappers off to zero for unchoked flow. Also, tests show that the tyre can be inflated from 1.0 bar to 3.0 bar in 8 s and deflated from 3.0 bar to 1.0 bar in 13 s. The APG bump tests and Belgian paving tests were conducted to validate the model over discrete obstacles and rough roads, respectively. These tests indicate that the model correlates with the actual trailer.

The validated model was used to develop the TIPc (Tyre Inflation Pressure controller), which uses a running RMS control strategy to manage the TIS. The objective of the TIPc is to maintain a *NOT uncomfortable* ride comfort level. The TIPc achieves this by deflating the tyre to a suitable tyre pressure when the ride comfort level is above *NOT uncomfortable*. The TIPc is robust to evaluate ride comfort on smooth roads and rough roads, as well as, detecting

© University of Pretoria

discrete obstacles. The TIPc ignores discrete obstacles when evaluating ride comfort to determine a suitable tyre pressure to improve ride comfort. The TIPc was able to achieve a $4 - 7\%$ RCI (Ride Comfort Improvement).

© University of Pretoria

Acknowledgements

A special thanks to the following people who made completion of this study possible, namely;

- **Prof P.S. Els** for the continuous guidance and advice throughout the study.
- VDG team (**C.M. Becker, T.R. Botha, G. Guthrie, H. Hamersma, W.C.W. Penny**) for;
  - The assistance and the knowledge shared;
  - Access to VDG facilities and equipment, and;
  - Assistance in conducting the tests.
- Family and friends (**L.M. Komana, L.B. Komana, T.M. Komana, C.N. Nchabeleng, M.K. Katsane**) for;
  - The continuous cheering and motivation you gave me;
  - Reading and commenting on the thesis;
  - All the love and support, and;
  - Special thanks to my parents (**M.J. Komana and R.D. Komana**), your principles are not lost on me.

© University of Pretoria

This page is intentionally left blank

© University of Pretoria

Table of Contents

© University of Pretoria

© University of Pretoria

List of Figures

© University of Pretoria

© University of Pretoria

© University of Pretoria

List of Tables

© University of Pretoria

LIST OF SYMBOLS

English symbols

-A	m^2	Area
-a	m/s^2	Tangential acceleration
-a_F	m/s^2	Front tangential acceleration
-a_R	m/s^2	Rear tangential acceleration
-a_n	m/s^2	W_b weighted acceleration vector
-a_{rms}	m/s^2	Acceleration rms
-Acc	m/s^2	Acceleration
-Az_RMS	m/s^2	Acceleration rms along the z axis
-$c_{bend\ in-plane}$	N/mm	Bending belt stiffness, in-plane
-$c_{bend\ out-of-plane}$	N/mm	Bending belt stiffness, out-of-plane
-c_{long}	N/mm	Longitudinal belt stiffness
-c_D		Discharge coefficient
-$c_{torsion}$	N/mm	Torsional belt stiffness
-F_x	N	Force along the x axis
-F_z	N	Force along the z axis
-g	m/s^2	Gravitational acceleration
-G_d	m^3	Displacement PSD
-I_{xx}	$kg\ /\ m^2$	Moment of inertia about the x-axis
-I_{yy}	$kg\ /\ m^2$	Moment of inertia about the y-axis
-I_{zz}	$kg\ /\ m^2$	Moment of inertia about the z-axis
-m_{cg}	kg	Mass (at the centre of mass)
-$\dot{m}_{choked}$	$kg\ /\ s$	Choked mass flow rate
-$\dot{m}$	$kg\ /\ s$	Mass flow rate
-$\dot{m}_{experimental}$	$kg\ /\ s$	Experimental mass flow rate
-$\dot{m}_{unchoked}$	$kg\ /\ s$	Unchoked mass flow rate
-$\dot{m}_{theoretical}$	$kg\ /\ s$	Theoretical mass flow rate
-n	$cycles/m$	Spatial frequency
-N		Number of points
-P^*	Pa	Critical pressure

© University of Pretoria

-$P_{absolute}$	Pa	Absolute pressure
-$P_{\text{atmospheric}}$	Pa	Atmospheric pressure
-P_{gage}	Pa	Gage pressure
-P_{i}	Pa	Tyre pressure
-P_1	Pa	Upstream pressure
-P_2	Pa	Downstream pressure
-r	m	Radius
-R	$J/mol \cdot K$	Gas constant
-r_F	m	Front radius
-r_R	m	Rear radius
-r_x		x-axis rotation
-r_y		y-axis rotation
-r_z		z-axis rotation
- RCI		Ride Comfort Improvement
- $R.E.\%$		Relative Error
-rms	m/s^2	Root Mean Square
-RMS	m/s^2	Root Mean Square
-rms_{long}	m/s^2	Long sampling distance rms
-$RMSo$	m/s^2	RMS overshoot
-rms_{short}	m/s^2	Short sampling distance rms
-$rms_{pressure\ controlled}$	m/s^2	Pressure controlled tyre rms
-$rms_{Passive\ at\ at\ 3bar}$	m/s^2	Passive tyre at 3.0 bar rms
-SF	Hz	Sampling frequency
-SD	m	Sampling distance
-T_1	K	Upstream temperature
-W_b		W_b frequency weighting
-W_c		W_c frequency weighting
-W_d		W_d frequency weighting
-W_e		W_e frequency weighting
-W_f		W_f frequency weighting
-W_g		W_g frequency weighting
-x		x-axis

© University of Pretoria

-x_{test}	Test value
-$x_{\text{simulation}}$	Simulation value
-y	y-axis
-z	z-axis

Greek symbols

-α	m/s^2	Angular acceleration
-Ω	rad/m	Angular spatial frequency
-∞		Infinity
- λ	m	Wavelength
- μ		Mean
-γ		Specific heat ratio
-σ		Standard deviation

List of Abbreviations

3	
-3D ENV	3D Enveloping Contact model
-3D VC	3D Equivalent Volume Contact model
A	
-ADAMS	Automatic Dynamics Analysis of Mechanical Systems (computer software)
-APG	Aberdeen Proving Ground
-ATIS	Automatic Tyre Inflation System
B	
-BES	Txuan Rotary Valve
-BS	British Standard
C	
-C++	C++ (Programming Language)
-CTIS	Central Tyre Inflation System
D	
-DAQ	Data Acquisition System

© University of Pretoria

-DOF	Degrees Of Freedom
F	
-FFT	Fast Fourier Transform
-FTire	Flexible Ring Tire Model
G	
-GPS	Global Positioning System
L	
-LH	Left hand
M	
-MATLAB	Matrix Laboratory (computer software)
-MPPES	Festo Proportional Pressure Regulator
-mppes	Festo Proportional Pressure Regulator
O	
-OPC	One Point Contact model
P	
-PSD	Power Spectral Density
R	
-RH	Right hand
-RMS	Root Mean Square
-rms	Root mean square
S	
-SIT	Self-Inflating Tyre
-std	Standard deviation
T	
-TIPc	Tyre Inflation Pressure controller
-TIS	Tyre Inflation System
-TPMS	Tyre Pressure Monitoring System
V	
-VDG	Vehicle Dynamics Group

© University of Pretoria

This page is intentionally left blank

© University of Pretoria

This page is intentionally left blank

© University of Pretoria

1 Introduction

This chapter discusses the motivation behind the development of a pressure controlled tyre to improve ride comfort. The background of the technology the study is based upon is discussed. The problem to be investigated is discussed and the objective defined. Then the contribution of the study to the field of vehicle engineering is discussed. The structure of the rest of the report is also given.

1.1 Background

Extensive research has been conducted over the years on the effect of the suspension system on handling and , more importantly for this study , ride comfort. Ride comfort and handling requirements are often in conflict, necessitating a compromise. Such studies have led to the development of smart suspension systems which have been commercialised in modern passenger vehicles. The objective of the smart suspension is to improve suspension performance by varying the suspension characteristics according to requirements. For handling performance the suspension is made ‘hard’, and for ride comfort performance the suspension is made ‘soft’. Commonly smart suspensions are categorised as semi-active and active. A discrete semi-active suspension switches between predetermined suspension characteristics to make the suspension ‘hard’ or ‘soft’ depending on the road inputs. Continuous variable semi-active suspension systems vary their characteristics continuously between ‘hard’ and ‘soft’ depending on the vehicle dynamics requirements.

Tyre Pressure Monitoring Systems (TPMS) have also been commercialised on modern vehicles. These systems monitor the tyre pressure and inform the driver when a tyre is under-inflated or over-inflated. Tyre Inflation Systems (TIS) have been commercialised on heavy vehicles to allow the driver to inflate or deflate the tyres from the cockpit to a suitable tyre pressure depending on the driving conditions. For example, in the military, TIS is used to improve the vehicle’s traction in off-road conditions. In the transportation industry TIS is used to reduce fuel consumption and reduce tyre wear. In the agriculture industry TIS is used to reduce operator fatigue and improve the ride comfort. However, in all cases the TIS require operator intervention to select one of the pre-defined tyre pressures.

It is widely known that tyre pressure has an influence on the tyre’s stiffness and damping characteristics. Therefore, smart suspension technology and TIS technology can be combined to control the tyre characteristics as the road conditions change to improve the vehicle’s ride comfort.

© University of Pretoria

1.2 Problem statement

Develop an automatic TIPc (Tyre Inflation Pressure controller) to improve ride comfort of vehicles on rough terrains without driver intervention.

1.3 Research objective

The aim of this study is to combine smart suspension control strategies with TIS technologies to develop a pressure controlled tyre to improve ride comfort for vehicles on rough terrains.

1.4 Research contribution

This study makes it possible to combine a pressure controlled tyre, smart suspension and smart anti-roll bar to improve high speed ride comfort and handling for vehicle, with a high centre of mass traveling on-road and off-road.

1.5 Research overview

This study is divided into 7 chapters:

Introduction: Outlines the purpose of the study and what the study intends to achieve.

Literature study: A summary of existing knowledge that is required to complete the study.

Model development and validation: A discussion of the model development and the tests conducted to verify that the model can accurately estimates the behaviour of the actual trailer.

TIPc development and implementation: The TIPc to improve ride comfort is developed and implemented on the trailer.

Conclusion: An evaluation of the performance of the pressure controlled tyre.

Recommendations: A discussion of possible avenues for future research with the new pressure controlled tyre capability.

References: List the sources of other people's work used in the study.

The process followed to complete this study is given in Figure 1-1. The process commences with the **Introduction** of the study. Followed by the gathering of relevant knowledge required to complete the study summarised in the **Literature study**, which is used in **Model development and validation** and **TIPc development and implementation**. **Model development and validation** involves developing the model to be used in the study. The

© University of Pretoria

model is simulated and if the simulation results are not satisfactory, then modification are made to the model, otherwise model validation tests are performed. If the model simulation and test results are not comparable, then modifications are made to the model, otherwise the process continues to **TIPc development and implementation. TIPc development and implementation** involves the TIPc logic development. Simulations are performed to evaluate the TIPc logic on the model. If the simulated TIPc performance is not satisfactory the TIPc logic is modified, otherwise the TIPc is implemented on the test trailer. TIPc implementation tests are conducted to evaluate the TIPc performance on the actual test trailer. If the implemented TIPc performance is not satisfactory the TIPc logic is modified, otherwise the process commences to the study **Conclusion** and **Recommendations.** A list of sources of knowledge used in the study is given in **References** to complete the study.

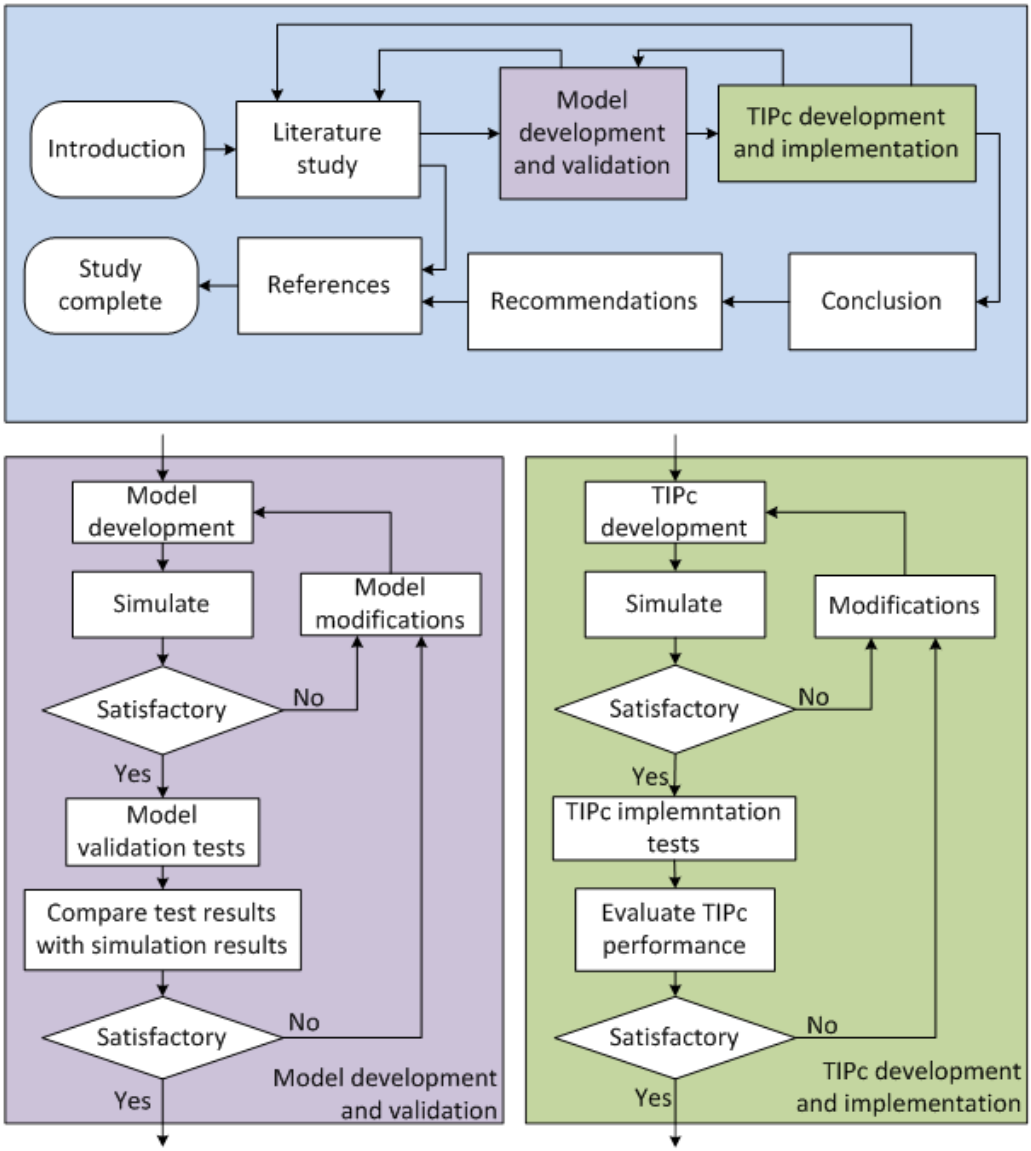

Figure 1-1 Thesis flow chart

© University of Pretoria

This page is intentionally left blank

© University of Pretoria

2 Literature study

This chapter discusses the foundation of knowledge that is relevant to conduct this study. This chapter is divided into six sections:

Section 2.1 discusses important tyre characteristics that are dependent on the tyre pressure. These tyre characteristics affect the vehicle performance. Special focus is placed on the tyre characteristics that affect ride comfort in the vertical direction. Different tyre models are discussed to identify an appropriate tyre model that yields the most accurate results for rough road simulations.

Section 2.2 discusses how terrain profile is measured and classified. Road classes range from smooth road to rough road.

Section 2.3 discusses the various TIS technologies that exist. Different industries have different objective for TIS technology, hence the different TIS technologies to meet the different industry needs.

Section 2.4 discusses the vehicle ride comfort. The vibration the vehicle experiences affect ride comfort, therefore causing discomfort to the occupants. Thus, engineers design suspension systems that minimise discomfort to humans.

Section 2.5 discusses smart suspension control strategies. This study does not focus on smart suspensions, however, smart suspension control strategies that improve ride comfort are of interest. These control strategies can be used to manage the tyre inflation pressure.

Section 2.6 discusses the mathematical modelling for tyre inflation and deflation.

Section 2.7 provides a summary of the relevant knowledge required to conduct the study.

© University of Pretoria

2.1 Tyres

Tyres are complex composite structures manufactured from a combination of many rubber and steel components. Tyres are the primary means of interaction between the vehicle and the road. The contact area between the tyre and the road is called the contact patch. All the tyre-road interaction forces are generated in the contact patch. These generated forces are responsible for the acceleration and braking of the vehicle, as well as cornering of the vehicle. In addition, the generated forces in the tyre-road interaction transmit the road irregularities to the vehicle. For these reasons tyre design and research is imperative.

This study only focuses on the tyre-road interaction, and how the generated forces in the tyre-road interaction influence the vehicle vertical dynamics.

2.1.1 Tyre stiffness and damping

Very simply put, a tyre is a spring and damper system absorbing road irregularities under a wide range of operating conditions, thereby helping provide a superior ride to the vehicle passengers (Khanse, 2015).

Tyres only work when in contact with the road. When a tyre loses contact with the road the tyre cannot generate the necessary forces to control the vehicle i.e. acceleration and cornering. In addition, when the tyre loses contact with the road the tyre cannot dampen the irregularities of the road, that is damping due to tyre deflection will not occur, thus, increasing the duration of vibration of the vehicle. For good ride comfort the tyre must maintain contact with the road (Adams, et al., 2004). As the tyre deforms, unwanted energy is dissipated and thus reduces the vibration transmitted to the vehicle.

The tyre stiffness and damping are inherent characteristics that are largely dependent on the tyre composition and tyre pressure. There are two tyre properties of interest for this study that are influenced by the tyre pressure, namely; tyre enveloping and ride comfort.

2.1.1.1 Tyre enveloping

It is practically impossible to create a perfectly flat road. Small irregularities will exist in the form of small bumps or small potholes. The tyre acts as a geometric filter smoothening the road irregularities, by deforming over the road irregularities. This property is known as the enveloping behaviour of the tyre, illustrated using the Tandem Elliptical Cam Model as shown in Figure 2-1 (Khanse, 2015).

© University of Pretoria

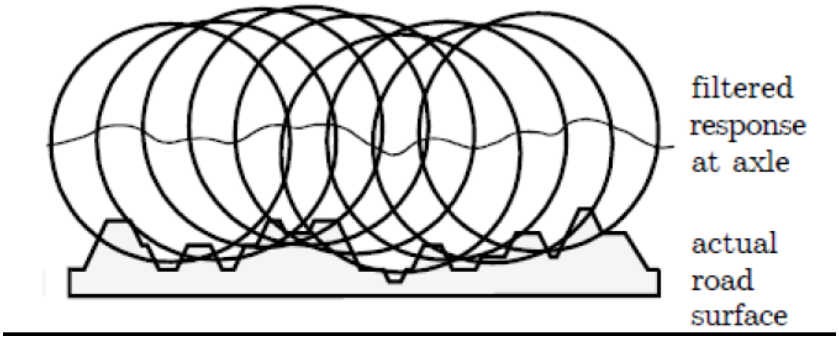

Figure 2-1 Tyre enveloping property (Khanse, 2015)

Research has shown that the shape of the elliptical cams does not change with tyre inflation pressure and that the tyre stiffness and contact length change cause the main effect (Besselink, et al., 2009). Besselink, et al. (2009) conducted a low speed enveloping test with fixed axle height and initial vertical force of 4000 N. The results from their study are shown in Figure 2-2 and Figure 2-3. As the tyre pressure is increased, the stiffness increases and the contact length becomes smaller resulting in larger forces and a shorter response. In contrast, as the tyre pressure decreases, the tyre damping increases and tyre deflection increases resulting more energy being dissipated and smaller forces being experienced.

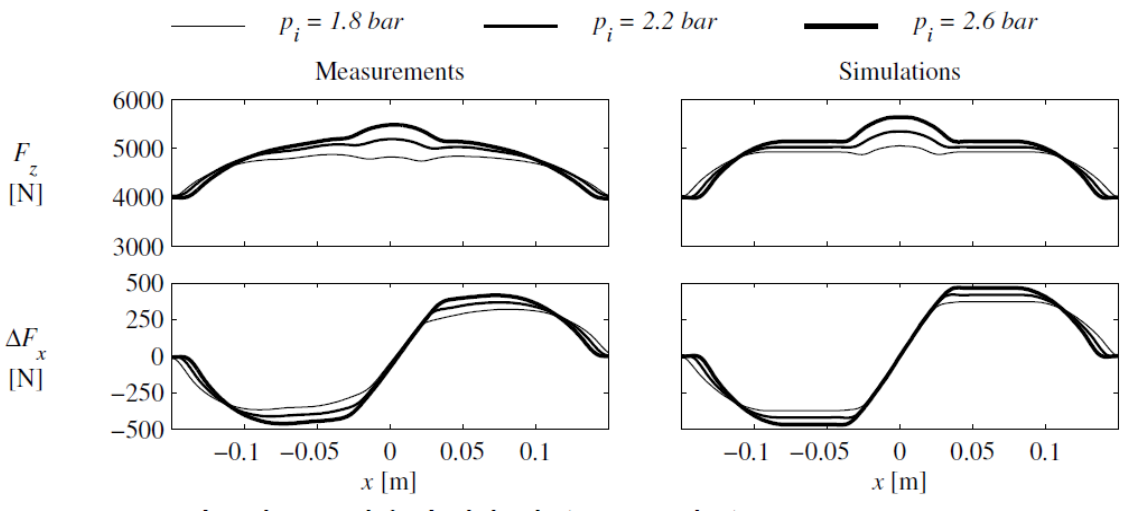

Figure 2-2 Low speed enveloping with fixed axle height (10x50 mm cleat) (Besselink, et al., 2009)

© University of Pretoria

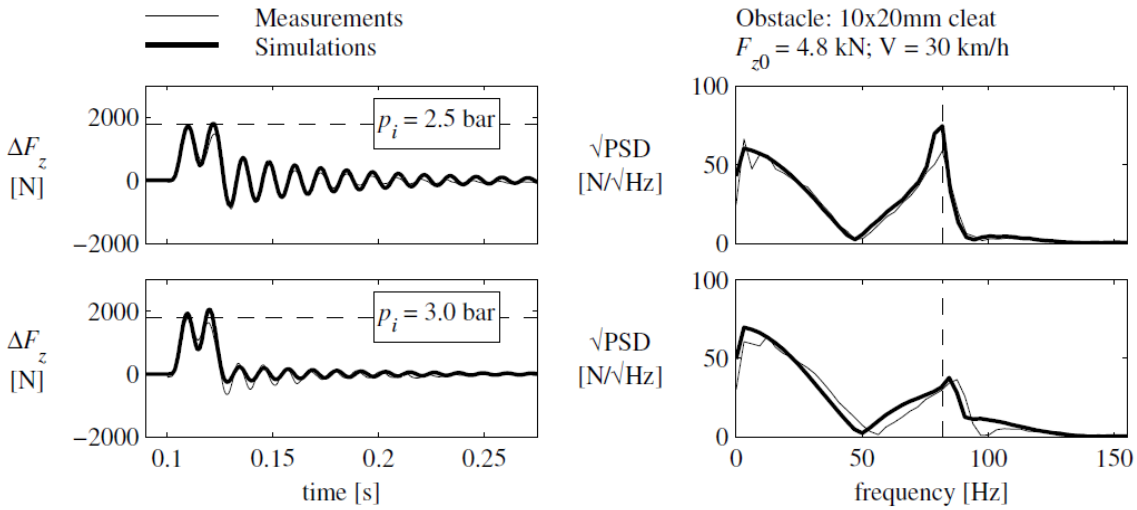

Figure 2-3 Cleat test of a passenger car tyre at a higher forward velocity (Besselink, et al., 2009)

According to Farroni & Timpone, (2016) as a tyre approaches an obstacle the tyre's contact patch makes contact with the obstacle before the wheel centre, because of its curvature in the contact zone. As the tyre rolls over the obstacle the wheel centre catches up and passes the obstacle before the tyre's contact patch passes the obstacle. The tyre's contact patch remains in contact with the obstacle after the wheel centre has passed the obstacle. This results in a tyre response that is much smoother than the obstacle shape as shown in Figure 2-4.

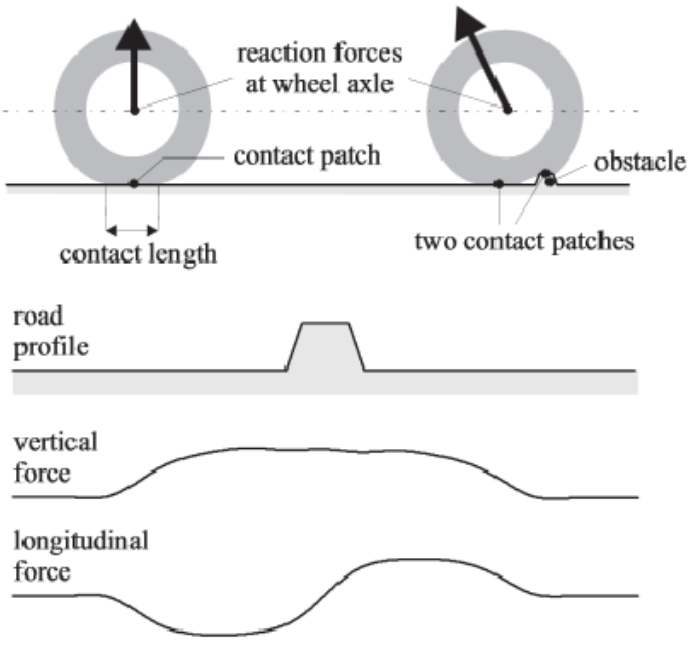

Figure 2-4 Tyre enveloping over a bump (Farroni & Timpone, 2016)

© University of Pretoria

2.1.1.2 Tyre pressure influence on ride comfort

Sherwin, et al. (2004) investigated the influence of tyre pressure on whole body vibration transmitted to the operator in a timber cut-to-length harvester. It was found there is no obvious trend in the vibration transmissibility corresponding to successive experimental tyre pressure settings (138, 345 and 414 kPa) for the lateral and longitudinal axes. However, vertical seat vibration transmissibility reduced significantly with a reduction in tyre inflation pressure.

Abdelghaffar, et al. (2014) found that vibrational tranmissibility in vehicles decreases when the tyre pressure is decreased. Figure 2-5 shows that for low frequency obstacles the vibrational transmissibility of a vehicle is marginally improved by reducing the tyre pressure. However, as the frequency increases reducing the tyre pressure significantly reduces the vehicle vibrational transmissibility. Vibrational transmissibility is not only dependent on the tyre pressure and tyre-road interaction, but is also dependent of the vehicle speed (Do Minh, et al., 2013).

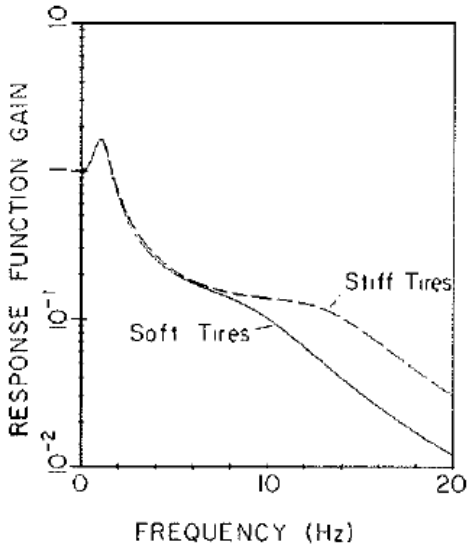

Figure 2-5 Effect of tyre stiffness on vehicle response function (Gillespie & Sayers, n.d.)

Do Minh, et al. (2013) states that tyres stiffness increases with increasing pressure, but at speeds lower than 10 km/h it remains constant. Conversely, tyre damping increases with decreasing tyre pressure and decreasing vehicle speed. Ride comfort is largely influenced by the suspension, however, the tyre influence on ride comfort cannot be ignored. If the spring stiffness becomes too high, the tyre stiffness will become dominant, negating the effect of the stiff spring (Uys, et al., 2007). The damping effect of tyres is small in comparison to the

© University of Pretoria

damping effect of the vehicle dampers (i.e. shock absorbers), but the tyre damping effect cannot be ignored (Abdelghaffar, et al., 2014).

There is a threshold to the minimum and maximum allowable tyre pressure. Reducing the tyre pressure past the tyre's threashold reduced the driver's control of the vehicle (Abdelghaffar, et al., 2014).

2.1.2 Tyre model

Tyres can be modelled numerically, empirically and symbolically. Numerical models such as Finite element tyre models offer high accuracy, but at a cost of expensive computation. Empirical models such as Pacejka tyre model require experimentally gained data used to parametrise the tyre. Data collection requires special test equipment. Symbolic models such as the Fiala tyre model is often the best choice for vehicle dynamic simulations, but for uneven roads a high fidelity contact model is required. However, when it comes to soft terrain, the tyre model needs to be extended to include the dynamics of the compliant ground (Petersen, 2009).

Cosin scientific software (2020) developed the FTire (Flexible Ring Tire Model) tyre model, which is based on structural dynamics. FTire is a robust tyre model that can be used for road and off-road vehicle dynamics and ride comfort simulations. The tyre belt is represented by a slim ring, that can be displaced and bent in arbitrary directions relative to the rim, including lateral direction (Gipser, n.d).

Gipser describes the tyre belt as one extensible and flexible ring carrying bending stiffnesses, elastically founded on the rim by distributed stiffnesses in the radial, tangential, and lateral direction. The degrees of freedom of this ring are such that rim in-plane as well as out-of-plane movements are possible. These belt elements are coupled with their direct neighbours by stiff springs and by bending stiffnesses both in-plane and out-of-plane. The radial stiffness is refined by a parallel connection of a spring with a spring-damper series connection to allow for dynamic hardening of the overall tyre radial stiffness at high wheel speeds. The tyre model describes the tyre belt as a very course, nonlinear finite element model. An in-plane and out-of-plane belt representation in FTire is shown in Figure 2-6.

© University of Pretoria

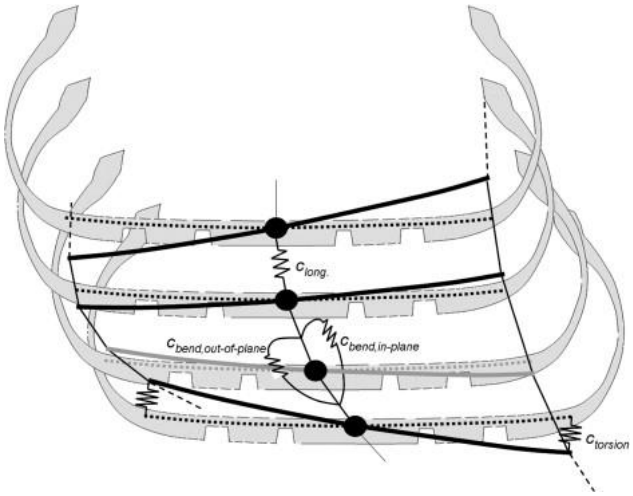

Figure 2-6 In-plane and out-of-plane belt representation in FTire (Taheri, et al., 2015)

All 6 components of tyre forces and moments acting on the rim are calculated by integrating the forces in the elastic foundation of the belt. The FTire model is accurate up to relatively high frequencies in the longitudinal, lateral and vertical directions. FTire deals with large and/or short-waved obstacles (Gipser, n.d).

Stallmann & Els (2014) summarise their investigation into the accuracy of tyre models for rough road simulations in Figure 2-7. They describe Belgian paving as a road surface that incorparates unevenness over a wide range of spatial frequencies, from the uneven block itself to unevenness that has a spatial frequency of a few meters. FTire gives the best results for simulation on rough roads and discrete obstacles. In addition, FTire is capable of changing the tyre inflation pressure during simulations, thus the tyre characteristics can be varied during simulation.

Group	Obstacle	Tyre model/ Contact model			
		FTire	3D ENV	3D VC	OPC
Discrete Obstacles	Cleats	Comparable, best	Comparable	Not representative	Not representative
	Trapezoidal bump	Comparable, best	Not representative	Comparable	Not representative
Rough tracks	Belgian paving	Comparable, best	Not representative	Comparable, under certain conditions	Not representative
	Fatigue track	Comparable, best	Not representative	Comparable	Not representative
	Parallel corrugations	Comparable, best	Not representative	Comparable	Not representative
	Angled corrugations	Comparable, best	Not representative	Comparable	Not representative

Figure 2-7 Tyre model summary (Stallmann & Els, 2014)

© University of Pretoria

2.2 Terrain

International Organization for Standardization 8608 (1995) is an international standard for reporting road surface profiles. The road profile is described as a displacement PSD (Power Spectral Density) or acceleration PSD.

The International Organization for Standardization 8608 classifies roads as shown in Figure 2-8. The road classes range from a Class-A road which is a smooth road, to a Class-H road which is very rough terrain. Becker (2008) profiled various roads at the Gerotek Test Facilities west of Pretoria, South Africa (Gerotek, 2020) with a Can-Can Machine. The Belgian paving is of particular interest, because Belgian paving can be used to investigate vehicle behaviour in rough road conditions. Becker (2008) found that the PSD of the Gerotek Belgian paving is approximately a Class D road. Hence, confirming that the Belgian paving as a rough road that can be used for off-road vehicle engineering investigations.

In contrast, Ward & Iagnemma (2009) uses acceleration data and speed data for road profiling. This approach requires prior knowledge of the vehicle suspension transmissibility. This method is robust enough to classify road profiles at different vehicle speeds and vehicle dynamic scenarios. On account of this, acceleration data can be used to identify a vehicle changing from one road to another, without accurately profiling the road if the suspension and tyre characteristics are unknown.

© University of Pretoria

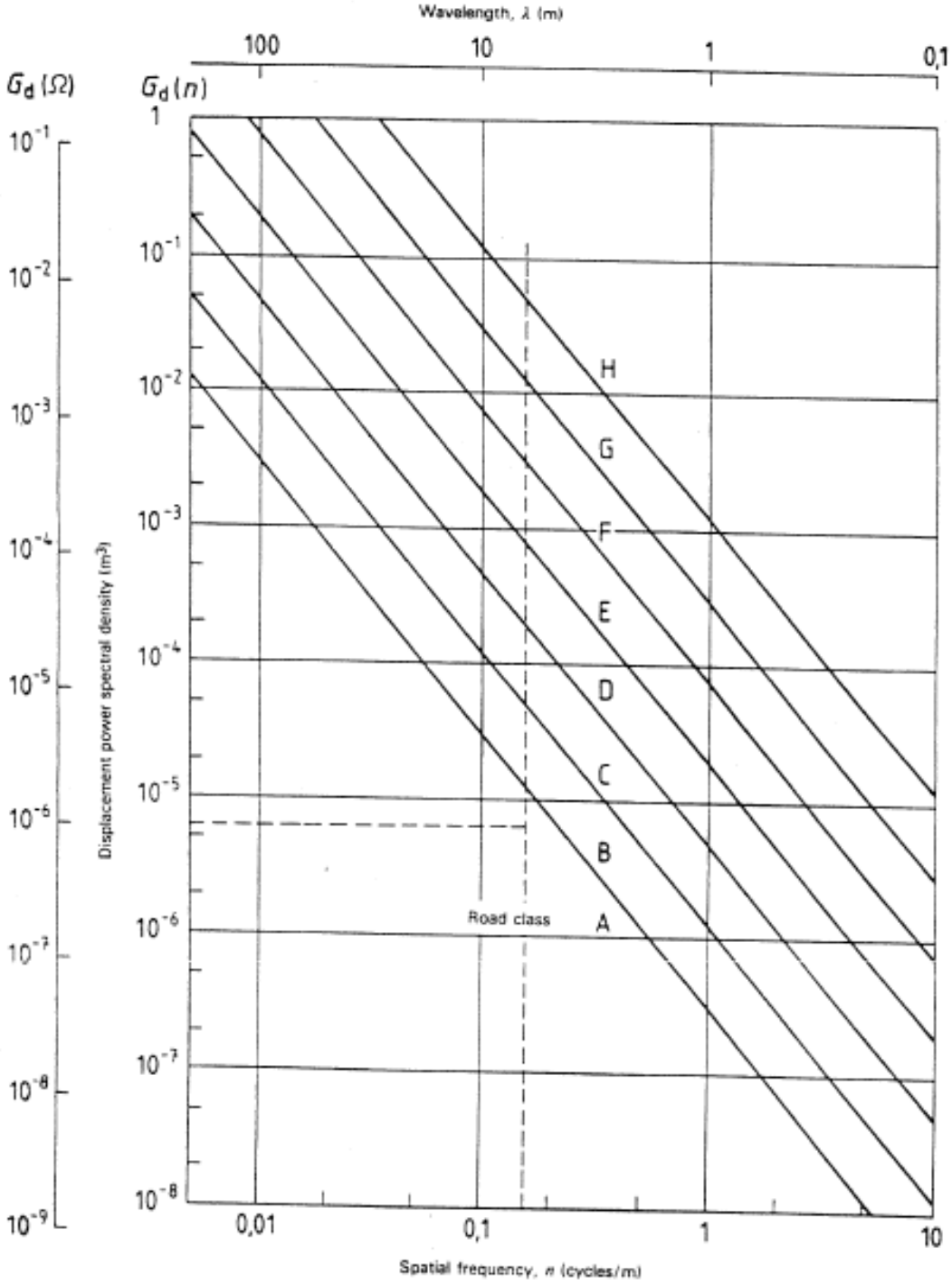

Figure 2-8 Displacement Spectral Densities for different classes of roads (International Organization for Standardization 8608, 1995)

© University of Pretoria

2.3 Tyre inflation systems

Tyres can be under inflated, correctly inflated or over inflated as shown in Figure 2-9. Under inflated tyres bulge upwards in the middle of the contact patch as shown in Figure 2-9(a). As a result, only the outer surfaces transmit the forces to the road. This leads to abnormal heating of the tyre which then causes damage to the tyre structure and shoulder wear. Under inflated tyres absorb more road irregularities and improves ride comfort. The flexibility in the sidewalls reduces the steering responsiveness. Over inflation reduces the tyre contact patch. The tyre contact patch narrows resulting in irregular tyre tread wear as shown in Figure 2-9(b). Also, over inflation makes the ride harsh, because the tyre is unable to effectively envelope the road irregularities. Ideally the tyre must make firm and even contact with the road at every point in the contact patch as shown in Figure 2-9(c).

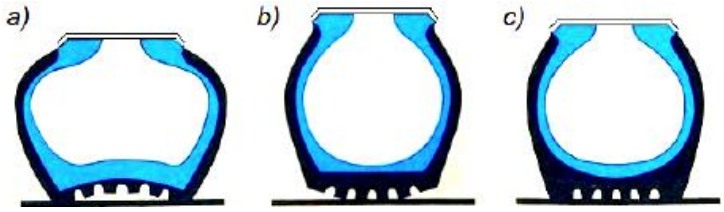

Figure 2-9 Inflation states (Caban, et al., 2014) (a) under inflation (b) over inflation, (c) correct inflation

Tyre inflation pressure is also dependent on the tyre temperature. As the tyre rolls over the road, heat is generated by the tyre leading to an increase in the tyre temperature. As tyre temperature increases, the air inside the tyre expands which results in an increase in the tyre pressure as shown in Figure 2-10.

A tyre can be correctly inflated before the journey. But, after a few kilometres of driving, the tyre pressure will be incorrect due to tyre heating. In racing, tyre pressure is measured when the tyres have reached steady state temperature after a few runs referred to as ‘target hot pressure’ (Wills, 2016).

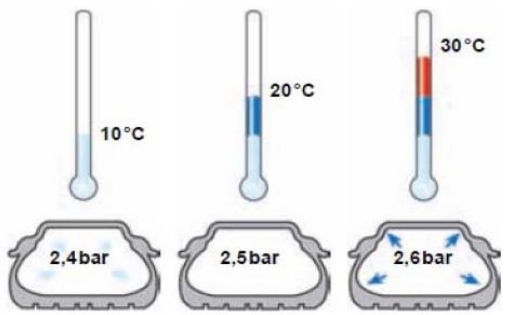

Figure 2-10 Inflation pressure dependence on temperature fluctuation (Caban, et al., 2014)

© University of Pretoria

Optimal tyre pressure benefits vehicle performance. Research has shown that tyre pressure has an influence on fuel consumption, tyre wear, overheating, road noise, acceleration and braking, handling and ride comfort. It is for this reason that it is advisable to check the tyre pressure daily to ensure that the tyre is inflated to the manufacturer's recommended tyre pressure.

Modern day vehicles are fitted with a TPMS that monitors the tyre pressure and informs the driver when the tyre pressure is not at the manufacturer's recommended tyre pressure. TPMS monitors tyre pressure directly or indirectly. Monitoring tyre pressure directly involves using a pressure sensor to measure the exact tyre pressure. Monitoring tyre pressure indirectly involves measuring other parameters to determine the tyre pressure, for example, monitoring the wheel angular speed. When wheel speeds are compared and any difference is an indication of under inflation. Indirect TMPS's are cheaper than direct TMPS's, but at the cost of accuracy and detection time. Moreover, preliminary statistical and simulation data show that an indirect TPMS can only detect half of existing under-inflations of 25% or more, because in some cases, under-inflation is undetectable in an indirect TPMS. For example, when two tyres are equally under-inflated. (Kubba & Jiang, 2014). TPMS can be battery powered referred to as an active system, or remotely powered to receive power wirelessly referred to as passive system.

A Central Tyre Inflation Systems (CTIS) allows the driver to change the tyre pressure from the cabin depending on the road condition. The main advantage of this system is to enable an increase of the traction of the vehicles when operating on soft roads. Therefore, it is widely implemented in fields such as construction, agriculture and military vehicles (Brondex, 2014). Decreasing the tyre pressure increases the contact area between the tyre and the road. As a result, the traction increases and the vehicle becomes less susceptible to sinkage in soft soil.

Automatic Tyre inflation System (ATIS) monitors the tyre pressure and automatically inflates the tyre when the pressure drops below the pre-set value. The system is able to compensate for slow leaks and punctures. The system is able to inflate rotating wheels on a steerable axle.

CODA DEVELOPMENT (2013) has developed a Self-Inflating Tyre (SIT) technology that allows the tyre to inflate itself without external support. The system relies on the peristaltic pump principles. In this respect, a tube chamber is integrated into the tyre wall when manufacturing the tyre. When the tyre rotates, the normal tyre deformation due to the vehicle

© University of Pretoria

weight presses the tube chamber at its lowest point. As the tyre rolls against the road, this lowest point moves along the peristaltic tube chamber forcing more air into the tyre with each wheel revolution. Once the optimum operating pressure is reached, an automatic pressure regulator disables the intake of atmospheric air and activates continuous internal air circulation within the peristaltic tube chamber (Brondex, 2014). Goodyear has also developed a SIT for large commercial vehicles. Figure 2-11 illustrates how the SIT works.

Figure 2-11 Self-Inflating Tyre (SIT) technology (Quick, 2012)

2.4 Ride comfort evaluation

Eriksson & Svensson (2015) define ride quality as a term describing a person's subjective perception of a vehicle ride. Poor ride quality gives rise to passenger discomfort and sometimes motion sickness. Comfort is a feeling of well-being while motion sickness is associated with dizziness, fatigue and nausea.

British Standards Institution 6841 (1987) is a standard used to evaluate the effect of vibration on the human body. Exposure to whole-body vibration causes oscillatory motions and force within the body. Vibration of the body may affect the acquisition of information via the sense, information processing, levels of arousal and activity.

Different parts of the body have different natural frequencies and different tolerances to vibration. At frequencies lower than 0.5 Hz vibration can cause motion sickness. The human

© University of Pretoria

body is very prone to discomfort at frequencies between 5-9 Hz. For this reason, suspension design aims to avoid the vehicle having a natural frequency in both frequency ranges.

Ride comfort is evaluated using acceleration rms (root mean square). The measured acceleration must be weighted with the appropriate weighting function before evaluation. The acceleration rms evaluation method is only usable when the crest factor is less than 6. The crest factor is calculated by Equation 2-1 (British Standards Institution 6841, 1987). However, Els (2005) found that the crest factor has little significance as far as the experience of ride comfort is concerned. On smooth roads (with a low rms value) a single peak caused by gear changes and brake application results in a high peak value, while the rms value is low.

Equation 2-1

$$Crest\ factor = \frac{weighted\ peak\ acceleration\ rms}{weighted\ acceleration\ rms}$$

The vertical acceleration measurements give the best, and in fact the only reliable measure for ride comfort (Uys, et al., 2007). For a seated vehicle occupant as shown in Figure 2-12 the measured vertical acceleration FFT (Fast Fourier Transform) is weighted with three weighting functions highlighted in Figure 2-13 when interested with the effects of vertical acceleration on the body. W_b is used when interested in the effects of vertical acceleration on human health, discomfort and perception. W_f is used when interested in the effects of vertical acceleration on motion sickness. W_g is used when interested in the effects of vertical acceleration on hand control and vision. In this study we will use only vertical acceleration as a measure of ride comfort.

© University of Pretoria

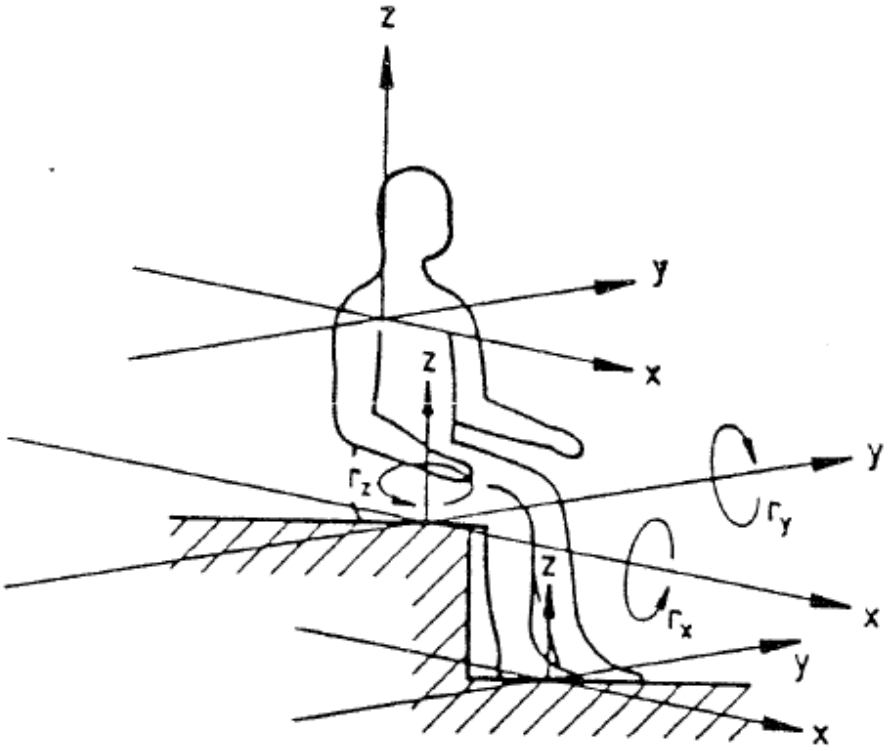

Figure 2-12 Principle basicentric axes for seated person (British Standards Institution 6841, 1987)

Table 1. Outline guide to the application of frequency weightings

Clause reference	4	5		6		7
Frequency weighting	Health	Hand control	Vision	Discomfort	Perception	Motion sickness
W_b	z-seat	–	–	z-seat x-, y-, z-feet z-standing vertical lying	z-seat – z-standing vertical lying	–
W_c	x-back	–	–	x-back	–	–
W_d	x-seat y-seat	x-seat y-seat	– –	x-seat y-seat x-, y-standing horizontal lying y-, z-back	x-seat y-seat x-, y-standing horizontal lying	–
W_e	–	–	–	r_x, r_y, r_z seat	–	–
W_f	–	–	–	–	–	z-vertical
W_g	–	z-seat	z-seat	–	–	–

Figure 2-13 Frequency weightings (British Standards Institution 6841, 1987)

© University of Pretoria

The steps to determine a vehicle's ride comfort is as follows;

1. The measured (or simulated) acceleration is transformed to the frequency domain.
2. W_b weighting is applied on the acceleration in the frequency domain. W_b weighting is shown in Figure 2-14.
3. The weighted acceleration is then transformed to the time domain.
4. Finally, the weighted acceleration in the time domain's rms value is calculated to determine the vehicle's ride discomfort level.
5. Crest factor is calculated to confirm whether the rms method can be used.

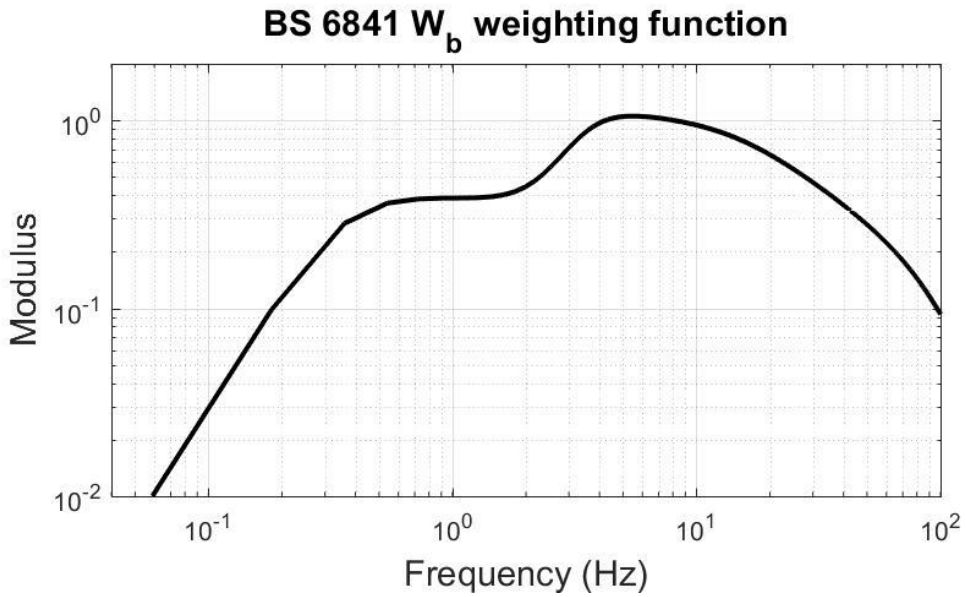

Figure 2-14 W_b weighting function

Figure 2-15 shows how the (British Standards Institution 6841, 1987) categorises levels of discomfort for a human exposed to whole body vibrations.

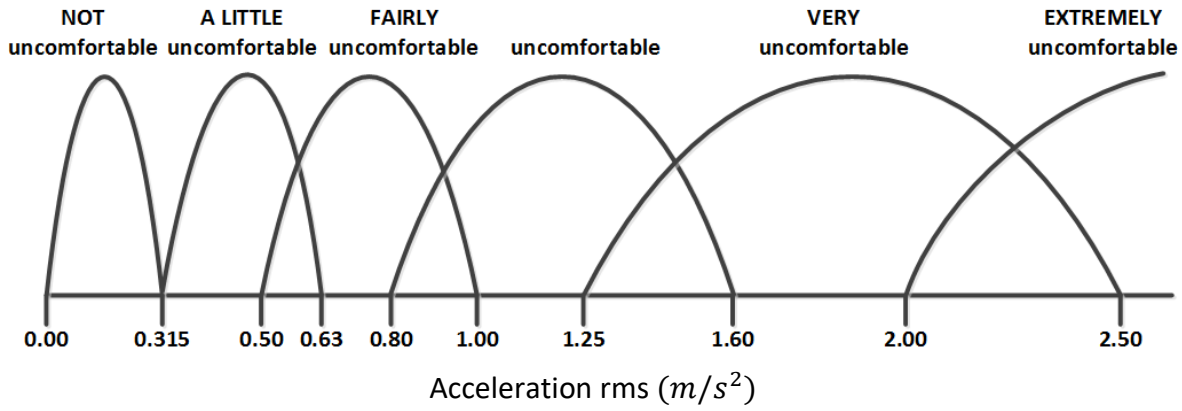

Figure 2-15 Discomfort levels (British Standards Institution 6841, 1987)

© University of Pretoria

2.5 Control strategies

2.5.1 Ride control

There are two main categories of disturbances experienced by a vehicle, road disturbance and load disturbance. Road disturbances are due to the road profile, and have the characteristics of large magnitude in low frequency (e.g. hills) and small magnitude in high frequency (e.g. off-road). Load disturbances are due to vehicle dynamic response, and are characterised by abrupt change (e.g. accelerating, braking, and cornering). Smart suspensions have been developed to minimise these disturbances to improve vehicle ride comfort. A suspension system with proper cushioning needs to be 'soft' against road disturbances and 'hard' against load disturbances (Mouleeswaran, 2012).

Smart suspension control strategies can be classified into two categories, input driven control and reaction driven control. Input driven strategies use parameters such as vehicle speed and steering angle as inputs to the controller. Reaction driven strategies use parameters such as yaw rate and roll rate as inputs to the controller. Therefore, input driven strategies react before a change is experienced. Conversely, reaction driven strategies react to change, that is, after a change has been experienced. Thus, input driven strategy reacts faster than a reaction driven strategy (Uys, et al., 2007).

Els (2006) implemented a running RMS (Root Mean Square) algorithm to control the switching between a soft suspension and hard suspension. The number of points in the running RMS influences the response time, threshold levels and rejection of noise for short duration events. The choice of running RMS duration is therefore a trade-off between response time and switching. The default suspension setting is 'soft' for normal driving to improve ride comfort performance. In an emergency manoeuvre such as a double lane change the controller switch the suspension to 'hard' for the duration of the manoeuvre to improve handling performance. Switching is not frequent and the strategy works well for on-road and off-road driving.

2.5.2 Terrain classification control

When changing terrain from on-road to off-road vehicle dynamic response such as vertical acceleration, roll and pitch give an indication of the change in terrain. The vertical acceleration, roll and pitch magnitudes will change abruptly. If the vehicle speed is not

© University of Pretoria

reduced, then passengers experience discomfort. It is more difficult to brace the human body against roll and pitch motion than is the case for yaw or vertical motion (Uys, et al., 2007).

Wang (2013) classifies the road in segmented intervals. After the vehicle has travelled over a particular length of the road the road detection system calculates the PSD for the segment to classify the road. The tests show that too small intervals increase the computational burden while too large intervals reduce the classification accuracy.

Some obstacles such as small stones are filtered by the tyre, but other obstacles such as potholes are not filtered by the tyre. Obstacles on the road are not representatives of the terrain type. Hence, obstacles must be removed before the terrain is classified. Ward & Iagnemma (2009) proposed an impulse detection method which is based on the hypothesis that the variation in a road profile should be relatively constant over a given terrain type. An obstacle will cause an abrupt and short variation. When an obstacle is detected the obstacle is removed from the road profile as shown in Figure 2-16.

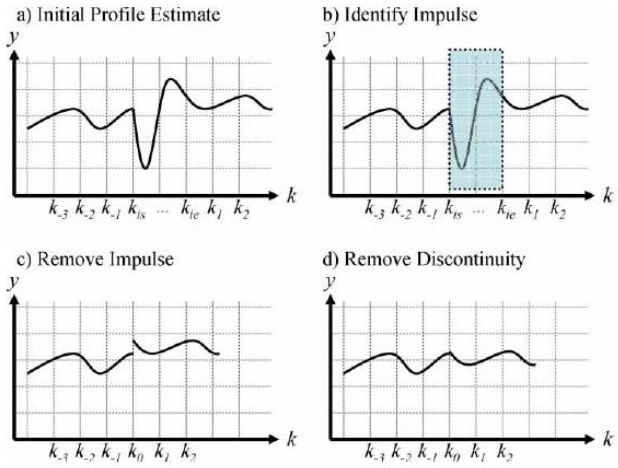

Figure 2-16 Obstacle detection (Ward & Iagnemma, 2009)

2.6 Tyre inflation and deflation

Brondex (2014) developed an adaptive tyre pressure system for vehicles that continuously regulates the tyre pressure for each wheel. According to Brondex (2014) the design of the pneumatic system to inflate or deflate a tyre is driven by the devices used to control the air flow, i.e. solenoid valve. Other parts of the pneumatic system such as fittings and piping are then selected such that they do not limit the solenoid valve performance.

Flow through a solenoid valve can be modelled as flow through an orifice. Flow through an orifice is nonlinear and can be divided into two main categories namely; unchoked flow and choked flow.

© University of Pretoria

Unchoked flow

Unchoked flow occurs when the downstream pressure is higher than the critical pressure. The critical pressure ratio is given by Equation 2-2. The critical pressure ratio is described by critical pressure (P^*), upstream pressure (P_1) and specific heat ratio (γ).

Equation 2-2

$$\frac{P^*}{P_1} = \left[\frac{2}{\gamma+1}\right]^{\left(\frac{\gamma}{\gamma-1}\right)}$$

$$\therefore P^* = \left[\frac{2}{\gamma+1}\right]^{\left(\frac{\gamma}{\gamma-1}\right)} P_1$$

The flow is unchoked when the downstream pressure is above the critical pressure as shown in Equation 2-3, where P_2 describes the downstream pressure

Equation 2-3

$$P_2 > P^*$$

Under unchoked flow conditions the mass flow rate is calculated by Equation 2-4. Unchoked mass flow rate ($\dot{m}_{unchoked}$) is described by the discharge coefficient (c_D), flow area (A), upstream pressure (P_1), gas constant (R), upstream temperature (T_1) and the specific heat ratio (γ).

Equation 2-4

$$\dot{m}_{unchoked} = c_D \frac{AP_1}{\sqrt{RT_1}} \sqrt{\frac{2\gamma}{\gamma-1}\left[\left(\frac{P_2}{P_1}\right)^{2/\gamma} - \left(\frac{P_2}{P_1}\right)^{\frac{\gamma+1}{\gamma}}\right]}$$

Choked flow

The flow is choked when the downstream pressure is below the critical pressure as shown in Equation 2-5.

Equation 2-5

$$P_2 \leq P^*$$

© University of Pretoria

Under choked flow conditions the choked mass flow rate ($\dot{m}_{choked}$) is calculated by Equation 2-6.

Equation 2-6

$$\dot{m}_{choked} = c_D \frac{AP_1}{\sqrt{RT_1}} \left[\frac{2}{\gamma+1}\right]^{\left(\frac{1}{\gamma-1}\right)} \sqrt{\frac{2\gamma}{\gamma+1}}$$

Figure 2-17(a) illustrates fluid flow through an orifice. Figure 2-17(b) illustrates the mass flow rate of a gas through an orifice as a function of the downstream-upstream ration $\frac{P_2}{P_1}$.

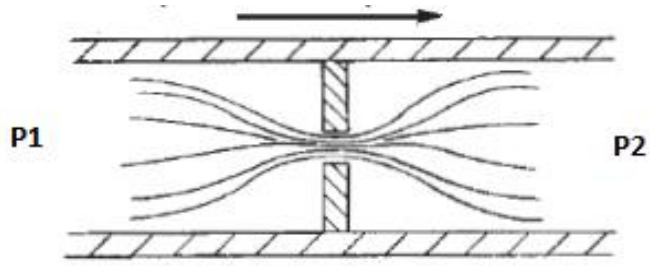

(a)

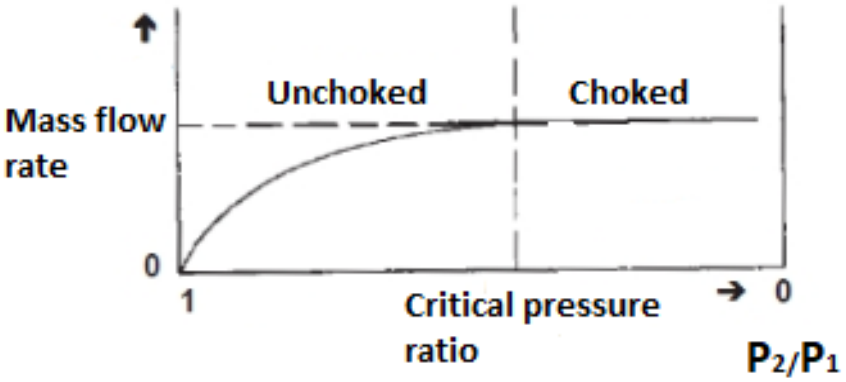

(b)

Figure 2-17 (a) Gas flow through an orifice (b) mass flow rate through a orifice (Jinhwan, 2013)

The discharge coefficient is a measure of efficiency of the pneumatic system. The discharge coefficient is a ratio of the actual mass flow rate ($\dot{m}_{experimental}$) to the theoretical mass flow rate ($\dot{m}_{theoretical}$) given by Equation 2-7.

Equation 2-7

$$c_D = \frac{\dot{m}_{experimental}}{\dot{m}_{theoretical}}$$

© University of Pretoria

2.7 Conclusion

Tyres are the primary interaction between the vehicle and the road with spring and damping characteristics that are dependent on the tyre pressure, allowing the tyre to deform over the road irregularities referred to as tyre enveloping. Decreasing the tyre pressure increases damping and improves the tyre enveloping behaviour responsible for filtering out road irregularities and dissipating unwanted energy resulting in an improvement in ride comfort performance. The tyre enveloping effect is more prevalent over discrete obstacles and rough roads.

Generally, for the purpose of this study, flat concrete paving is classified as a smooth road, while Belgian paving is classified as rough road. The FTire tyre model is an accurate model for both smooth and rough road simulations, with the capability of changing the tyre pressure during simulation. Acceleration data can be used to detect a change in the terrain and a discrete obstacle in the road without accurately profiling the road. However, a method of differentiating between road inputs from vehicle dynamic response is required to solely use acceleration data for terrain change and discrete obstacle detection.

TIS ensure that tyres are maintained at the correct inflation pressure. TIS's pneumatic system can be mathematically modelled as nonlinear gas flow through an orifice, under choked or unchoked conditions depending on the upstream/downstream pressure ratio. Correct inflation pressure can be based on improving ride comfort to reduce human exposure to whole body vibrations resulting in discomfort. Vertical acceleration rms is a reliable method of determining the human ride comfort. A running RMS controller is a simple and robust suspension control strategy to improve ride comfort.

The literature study indicates that with the existing knowledge, it is plausible to combine a smart suspension control strategy with a TIS to improve ride comfort over rough roads. The TIS can be modelled as a flow through an orifice when inflating and deflating the tyre. And, a running RMS control strategy can be used to manage the TIS, to vary the tyre characteristics as the road condition changes to improve ride comfort. Chapter 3 discusses the development of the vehicle model, capable of changing the tyre pressure through a TIS during simulation used in this study. Chapter 4 discusses the development of a TIPc that uses a running RMS control strategy to evaluate the ride comfort, to determine a suitable tyre pressure to improve ride comfort.

© University of Pretoria

This page is intentionally left blank

© University of Pretoria

This page is intentionally left blank

© University of Pretoria

3 Model development and validation

This chapter discusses the VDG (Vehicle Dynamics Group) test trailer model used in this study, as well as the tests conducted to validate that the trailer model accurately represents the behaviour of the actual trailer.

Section 3.1 discusses the model created to simulate the behaviour of the actual trailer. The trailer model can inflate and deflate the right tyre of the trailer while the trailer is moving. The trailer model consists of 5 sub-models namely:

1. Body model;
2. Pneumatic system model;
3. Tyre model;
4. Suspension model; and
5. TIPc model;

Section 3.2 discusses the tests conducted to verify that the trailer model accurately represents the behaviour of the actual trailer. Three different tests were conducted to parametrise and validate the simulation model, these tests include:

1. Pneumatic system parametrisation tests;
2. APG (Aberdeen Proving Ground) bump tests; and
3. Belgian paving tests;

3.1 Model development

The trailer model is a combination of differential and algebraic equations to closely estimate the trailer behaviour. The trailer is modelled on 3 platforms, namely; ADAMS (Automatic Dynamics Analysis of Mechanical Systems) View, Cosin, and MATLAB (Matrix Laboratory). Simulink (MATLAB-based graphical programming environment) is used to manage the co-simulation between all 3 platforms.

ADAMS is used to solve the body multi-dynamics equations. Cosin is used to compute the tyre-terrain interaction. MATLAB and Simulink are used to calculate the suspension forces, as well as to develop the TIPc discussed in section 4.1 (TIPc development).

© University of Pretoria

3.1.1 Simulink and MATLAB

Figure 3-1 shows the trailer model used in the study, as well as how the sub-system models interact with each other. A velocity is applied to the body model. The body model calculates the suspension displacements and velocities, and these body model outputs are used by the suspension model as inputs. The body model also calculates the wheel position and orientation, and these body model outputs are used by the tyre model as inputs. Additionally, the tyre model receives as input the instantaneous right tyre pressure calculated by the pneumatic system model. The body model calculates the rear acceleration and the longitudinal displacement, and these body model outputs are used by the TIPc model as inputs.

The suspension model calculates the suspension forces given the suspension displacement and velocity. The suspension model outputs are then fed to the body model as inputs. The tyre model calculates the tyre forces and moments given the wheel position and orientation. The tyre model outputs are fed to the body model as inputs. The TIPc determines the most suitable tyre pressure based on the rear acceleration and longitudinal displacement. The TIPc output is fed to the pneumatic system as an input. The pneumatic system model calculates the tyre and tank instantaneous pressures as the tyre is inflated or deflated to reach the tyre pressure selected by the TIPc. The pneumatic system model output is fed to the tyre model. Further discussion on the TIPc model is given in chapter 4.

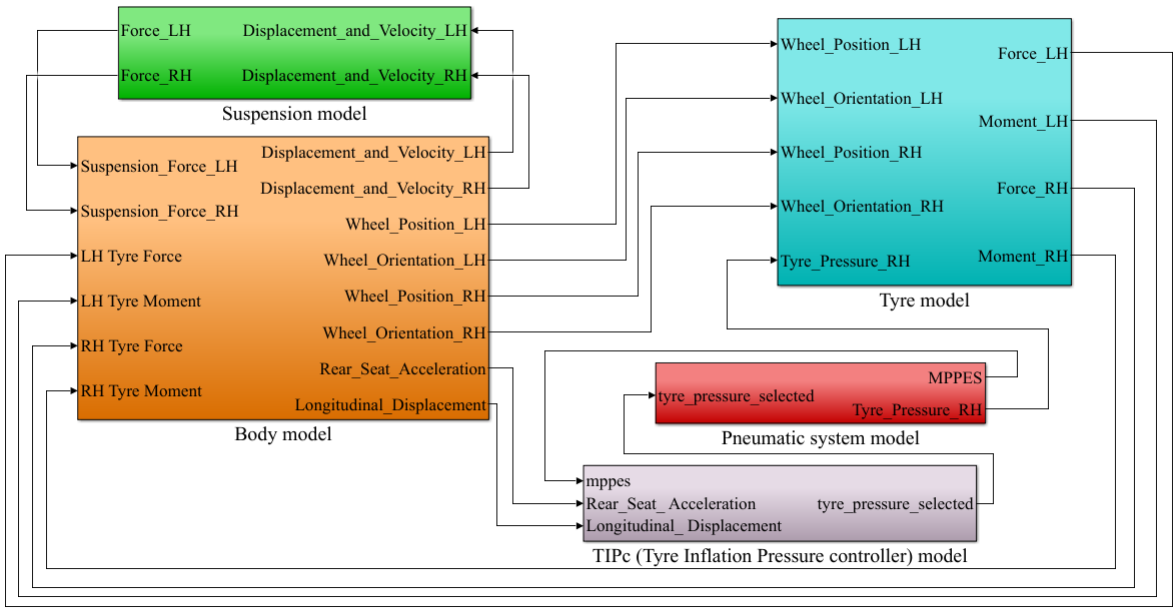

Figure 3-1 VDG test trailer model in Simulink

© University of Pretoria

3.1.2 Body model

The body model is shown in Figure 3-2. The body model consists of the following:

- Chassis (1) with a tow hook (2) in the front;
- An unsteerable axle (3) attached to the chassis by a trailing arm and A-frame. The suspension (spring and damper) is modelled outside of ADAMS;
- A rim (4) on either side of the axle. The rim does not have a tyre, because the tyre is modelled outside of ADMAS; and
- Square body (5) fixed on top of the chassis. The square body represents the vehicle body;

A longitudinal velocity is applied to the tow hook. This represents the speed applied to the test trailer by the towing vehicle through the tow hook. The tow hook has 4 DOF (Degree Of Freedom). The tow hook is free to rotate about all axes and free to translate along the longitudinal axis.

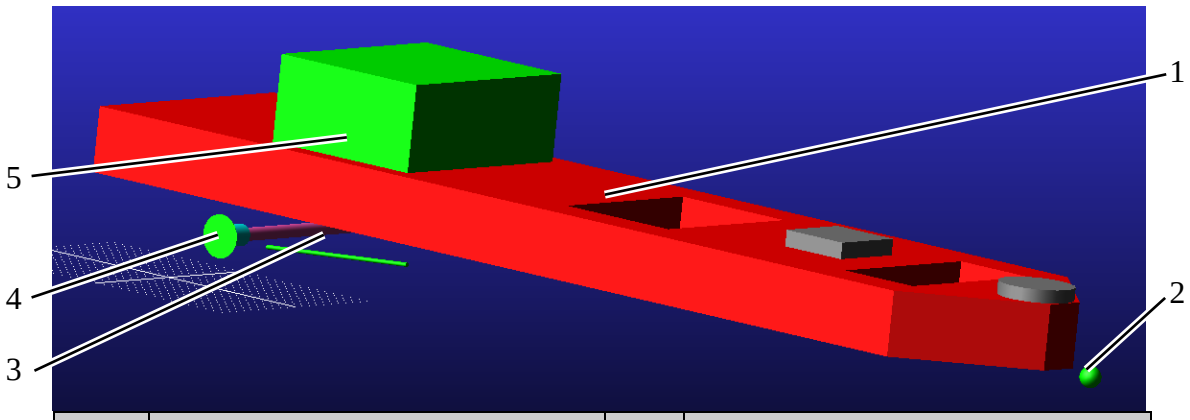

1	Chassis	**2**	Tow hook
3	Axle	**4**	Rim
5	Square body		

Figure 3-2 Body model

A summary of important characteristics of the trailer body are given in Table 3-1.

Table 3-1 Trailer body characteristics (body model) (Žuraulis, et al., 2017)

$I_{xx}(kgm^2)$	295.21
$I_{yy}\ (kgm^2)$	996.65
$I_{zz}\ (kgm^2)$	4701.88
$m_{cg}\ (kg)$	1027

© University of Pretoria

3.1.3 Tyre model

Cosin uses the FTire model for tyre-terrain interaction computation. Cosin requires 2 files, a terrain file and a tyre file. Three different terrains were used; namely, an APG bump, concrete paving (smooth road) and Belgian paving (rough road) prepared by Becker (2008), and a Michelin LTX AT2 tyre file prepared by Bosch (2016) is used. Table 3-2 summaries important tyre characteristics.

Table 3-2 Trailer tyre characteristics (tyre model)

$I_{xx}(kg/mm^2)$	1.011		
$I_{yy}\ (kg/mm^2)$	2.022		
$I_{zz}\ (kg/mm^2)$	1.011		
$m_{cg}\ (kg)$	13.63		
$Wheel\ size$	$235/\ 85/R16$		
Tyre pressure (bar)	$1.25 - 3.0$		
Tyre volume (L)	66		
Terrain	APG bump	Concrete paving	Belgian paving

3.1.4 Pneumatic system model

The trailer pneumatic system is shown in Figure 3-3. The pneumatic system is used to inflate and deflate the trailer's right tyre to a tyre pressure determined by the TIPc. High pressure nitrogen gas at 9 bar is stored in the tank. A sensor block is mounted to the tank. A thermocouple and pressure transducer on the sensor block is used to measure the tank gas temperature and pressure respectively. To inflate the tyre the MPPES (Festo Proportional Pressure Regulator) is opened. Then high pressure gas from the tank flows through the MPPES to the second sensor block. A thermocouple on the sensor block is used to measure the temperature of the gas between the MPPES and the BES (Txuan Rotary Valve). From the sensor block the high pressure gas flows through the BES to the tyre.

The BES allows the tyre to be inflated or deflated while the tyre is rolling without twisting the piping. The BES consists of a stationary part and a rotating part. The stationary part is fixed and connected to the stationary sensor block. The rotating part is connected to the rotating wheel hub. A hollowed drive shaft is used to transmit the wheel rotation to the BES, so that the BES's rotating part rotates at the same speed as the wheel. A pressure transducer on the tyre is used to measure the tyre pressure. The pneumatic system is completed with pipes and fittings that are used to connect the components discussed.

© University of Pretoria

The MPPES inflates the tyre by opening to allow the high pressure gas from the tank to flow to the tyre. To deflate the tyre the MPPES is opened to the atmosphere, allowing the high pressure gas in the tyre to be released into the atmosphere as shown in Figure 3-4.

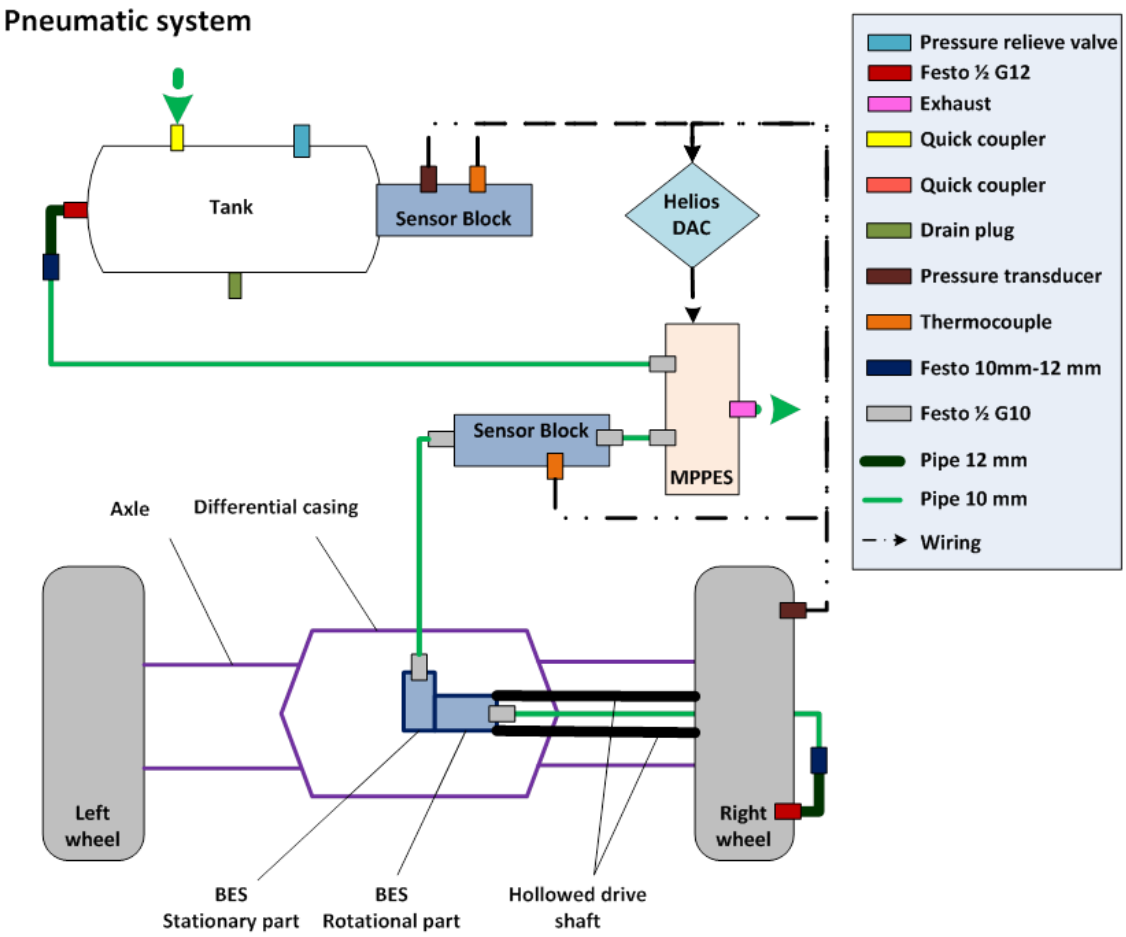

Figure 3-3 Pneumatic system

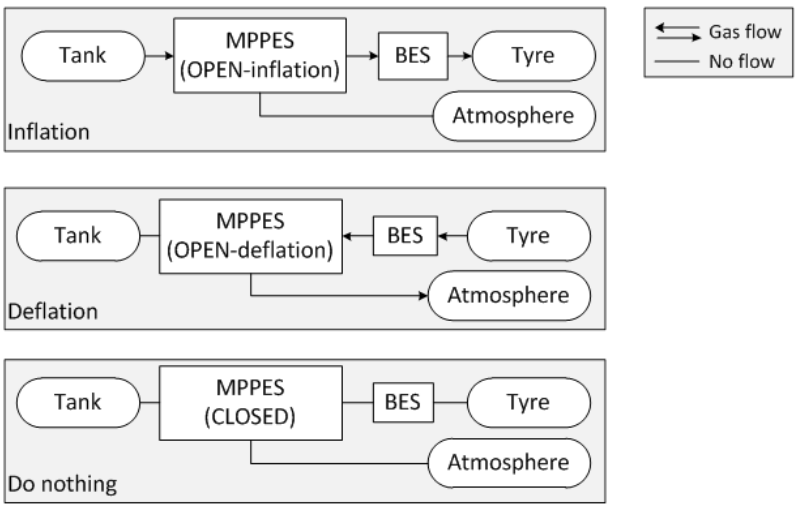

Figure 3-4 Pneumatic system flow diagram

© University of Pretoria

A summary of important characteristics of the pneumatic system are given in Table 3-3.

Table 3-3 Pneumatic system characteristics (pneumatic system model)

Tank volume (L)	90	
Tank max pressure (bar)	10	
Tyre volume (L)	66	
Pipe internal diameter(mm)	7.1	9.2
MPPES internal diameter(mm)	8	
BES internal diameter(mm)	8	

3.2 Model validation tests

Extensive work has been conducted by Žuraulis, et al., (2017) to validate the trailer model. However, modifications made on the trailer require that the modified trailer model be re-validated. The modifications include the pneumatic system and the tyre model. Žuraulis, et al., (2017) did not require in-situ tyre inflation, therefore a pneumatic system was not required. As a result, their tyre model could be implemented directly in ADAMS. To allow for in-situ tyre inflation the tyre model is modified and is instead modelled using Cosin FTire. Therefore, validation of the modified trailer is limited to the modifications made.

Tests under the same conditions are performed more than once to ensure repeatability of the results.

3.2.1 Test equipment

The test equipment used in this study includes 8 sensors, 1 data recorder and 1 telemetry. Table 3-4 list the equipment used. A pressure transducer and thermocouple are used to directly measure the tank pressure and temperature respectively. These sensors are placed opposite the tank outlet to minimise the dynamic pressure component on the measured pressure. Three accelerometers are used to measure the acceleration on the wheel, rear spring and damper mount and on the trailer where the front seats would be located. A thermocouple placed between the MPPES and BES is used to indirectly measure the tyre temperature. A pressure transducer on the tyre is used to directly measure the tyre pressure. Again, to minimise the dynamic pressure component the pressure transducer is placed as far a possible from the tyre inlet. A GPS (Global Positioning System) is used to measure the trailer speed. A DAQ (Data Acquisition System) is used to record the sensor measurements. All these sensors except the tyre pressure transducer are connected directly to the DAQ. To prevent the

© University of Pretoria

tyre pressure transducer cable from twisting as the tyre rolls, the tyre pressure transducer is connected to the telemetry and the telemetry is connected to the DAQ.

Table 3-4 Test equipment

Equipment	Equipment name	Measurement range
Tank pressure transducer	WIKA S-10	$0 - 25\ bar$
Tyre pressure transducer	Kyowa PGL-A-1MP-A	$0 - 1MPa$
Wheel acceleration	Crossbow CXL10 LP3	$\pm 10g$
Rear acceleration	MEMSIC GL10GP3	$\pm 10g$
Front acceleration	Crossbow CXL04 LP3	$\pm 4g$
Tank thermocouple	WIKA TC40	$-40 - 1200℃$
Tyre thermocouple	WIKA TC40	$-40 - 1200℃$
GPS	U Blocks 8M	$0 - 100\ km/h$
Telemetry		
DAQ	Diamond Systems Helios Single Board Computer	

3.2.2 Calibration

The test equipment used for the experiments are calibrated to ensure that the test results are reliable. For the results to be considered reliable, the test results must be accurate and precise. Accuracy is a measure of the correlation between the actual value and the measured value. Precision is a measure of correlation between multiple measurements with each other.

Calibrating ensures that measurements are accurate and within an acceptable limit, by determining the linear relationship between the sensor voltage measurement and the actual measure quantity. Thus, calibration is necessary to determine a function to relate sensor voltage measurements to the control measurements.

3.2.3 Model parametrisation and validation

Trailer model simulation results are compared to the test results to evaluate the accuracy of the model. Inaccuracies can be attributed to the test equipment, simplification of the model and numerical approximation during the model computation.

Test equipment inherently experience unavoidable noise such as circuitry noise, electromagnetic interference and radio frequency interference in the sensors, DAQ and wiring.

© University of Pretoria

In reality the trailer is towed by a vehicle with a suspension, but the tow vehicle is not included in the model to reduce the computing cost. The model is simplified by giving the tow hook in the trailer model 4 DOF. All rotations around the tow hook and longitudinal translation motions are allowed, but the tow hook model does not have vertical and lateral translations. In reality the tow vehicle applies 6 DOF to the trailer through the tow hook. The model was simplified to 4 DOF, because the lateral displacement and vertical displacement of the tow hook were considered negligible. The tow hook lateral displacement is assumed to be negligible, because the tow vehicle follows a straight path. The tow hook vertical displacement is assumed to be negligible, because the tow vehicle's vertical translation is negligible in comparison the vertical displacement of the trailer suspension. These assumptions are not necessarily valid over rough terrain, also the mount of the trailer will apply forces to the tow hook of the towing vehicle.

3.2.3.1 Pneumatic system parametrisation tests

In this section the tyre pressure or tank pressure are discussed in terms of gage pressure, but the gas equations discussed refer to absolute pressure. The absolute pressure ($P_{absolute}$) is the sum of the atmospheric pressure ($P_{\text{atmospheric}}$) and the gage pressure (P_{gage}) as described in Equation 3-1. The normal atmospheric pressure at the test location is $87876.5\ Pa$.

Equation 3-1

$$P_{absolute} = P_{\text{atmospheric}} + P_{gage}$$

The modelling of the pneumatic system was subject to the assumptions discussed below.

Assumptions

- Inflation gas (air and nitrogen) is an ideal gas;
- Tyre volume is constant;
- Solenoid is fully open;
- No external work is done on the system;
- Adiabatic gas process (no heat transfer with environment); and
- The volume of the pipes and fittings can be neglected;

Inflation and deflation tests

The goal with the inflation tests is to determine the time to both inflate the tyre from state 1 to state 2 and deflate the tyre from state 2 to state 3.

© University of Pretoria

To inflate the tyre, air must flow from the high pressure tank to the tyre at a lower pressure. To deflate the tyre, high pressure air in the tyre must be released to the atmosphere at a lower pressure. Fluid flow is due to a pressure differential between two points. Fluid flows from a higher pressure point (upstream) to a lower pressure point (downstream). The mass flow rate is dependent on the instantaneous pressure and temperature of the tank, tyre and atmosphere.

Figure 3-5 shows the tank pressure and tyre pressure as the tyre is inflated and deflated. As the tyre pressure increases the tank pressure decreases. The tank and tyre pressure were measured and used to simultaneously determine the pneumatic system discharge coefficient and fluid's mass flow rate of the pneumatic system using Equation 2-2 - Equation 2-7. Numerical analysis was used to determine the mass flow rates and discharge coefficient as shown in Figure 3-6. Firstly, it can be seen that the 'Theoretical mass flow rate' is greater than the 'Test mass flow rate'. It can be seen that the 'Test mass flow rate' is zero beyond a 'Tyre Pressure/ Tank Pressure' ratio of 0.8, in contrast to the 'Theoretical mass flow rate' that is only zero when the 'Tyre Pressure/ Tank Pressure ratio' is 1.This is as a result of the MPPES continuously switching between open and closed when the downstream pressure and upstream pressure are close. The discharge coefficient is approximately 0.07 when the flow is choked and tappers off to zero when the flow becomes unchoked.

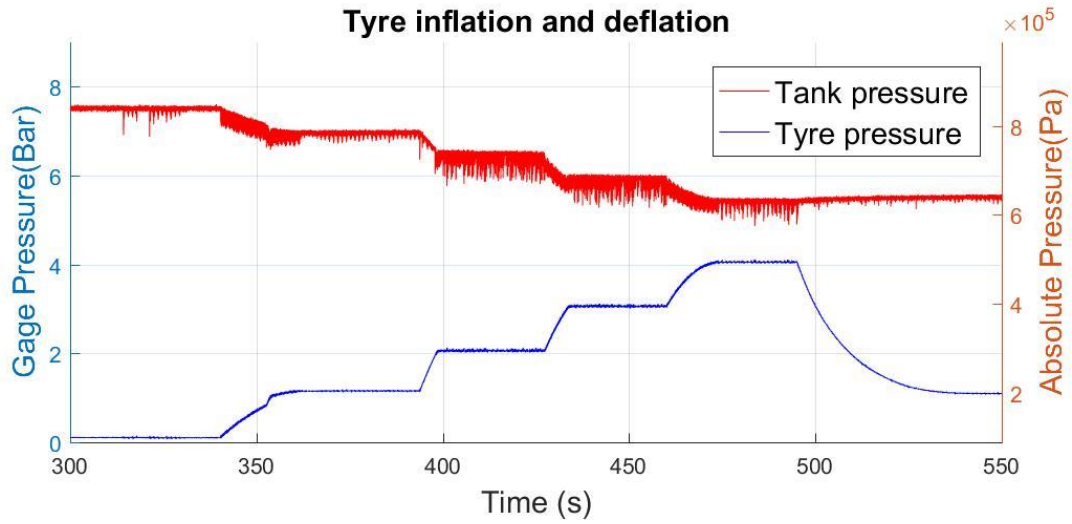

Figure 3-5 Test results - tyre pressure and tank pressure

© University of Pretoria

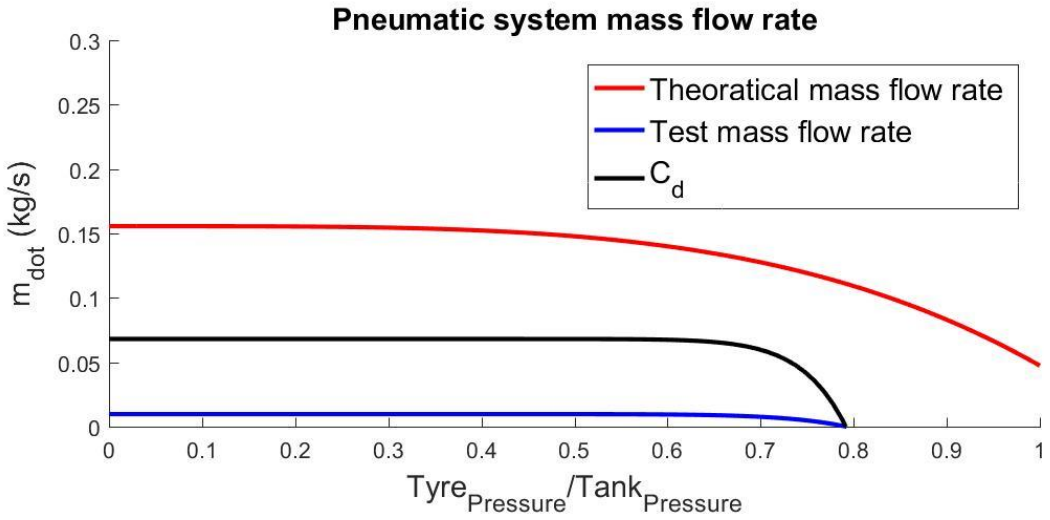

Figure 3-6 Pneumatic system mass flow rate and discharge coefficient

Figure 3-7 compares the pneumatic system model to the test results for inflating the tyre from 0.0 bar to 3.0 bar and deflating the tyre back to 0.0 bar. There is a close correlation between the pneumatic system model and the test results. It can be seen that when the tyre is fully deflated the gage pressure scale reads 0 bar and the absolute pressure scale reads 87876.5 Pa. It takes 8 s to inflate the tyre from 1.0 bar to 3.0 bar and 13 s to deflate the tyre from 3.0 bar to 1.0 bar.

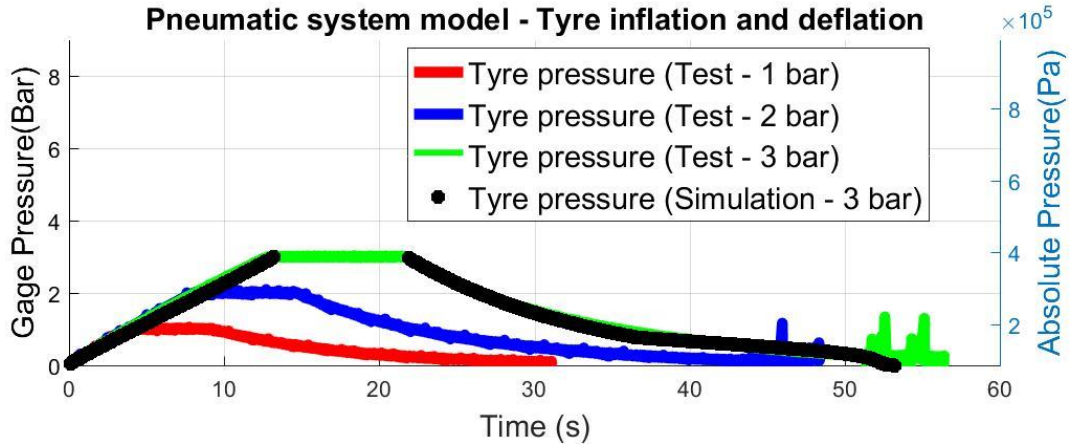

Figure 3-7 Pneumatic system model

3.2.3.2 APG Bump validation tests

Three APG bump tests were conducted to validate the body model and tyre model. The three APG bumps used are shown in Figure 3-8, where the dimensions are described in mm. A total of 12 APG bump tests were conducted which are summarised in Table 3-5. Each test was repeated to ensure repeatability resulting in a total of 24 APG bump tests.

© University of Pretoria

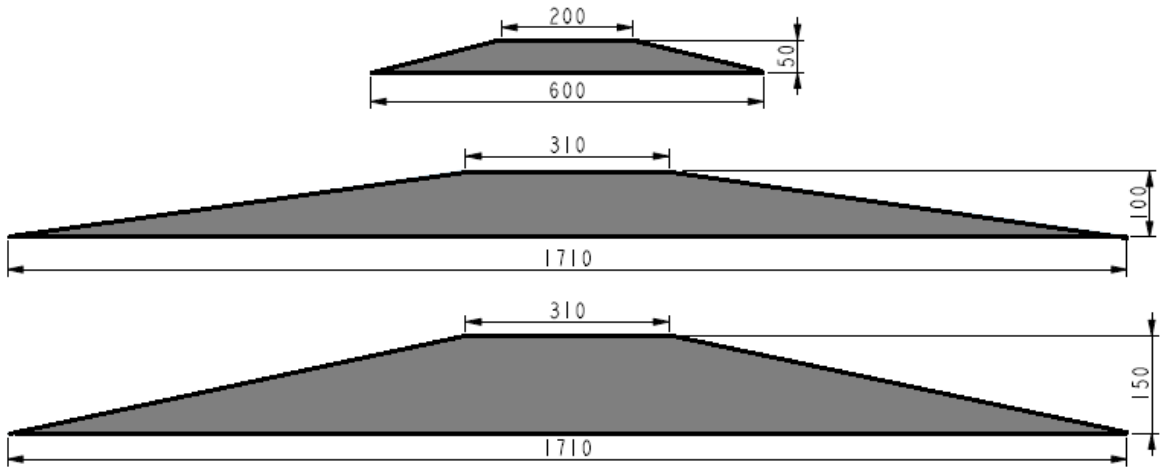

Figure 3-8 APG bumps

Table 3-5 APG bump tests conditions

APG bump	Speed	Tyre pressure		
		1.25 *bar*	**2.0 *bar***	**3.0 *bar***
50 *mm*	10 km/h	✔	✔	✔
100 *mm*	10 km/h	✔	✔	✔
	20 km/h	✔	✔	✔
150 *mm*	10 km/h	✔	✔	✔

The APG bump test can be divided into 3 sections, namely; before the bump, in contact with the bump and after the bump. To validate the model's response to tyre excitation, focus is on the section when the tyre is in contact with the APG bump (Stallmann, 2014). To ensure that the test results are useful to validate the model, the tyre must remain in contact with the APG bump as the tyre rolls over the bump. The test trailer was towed over the APG bump at speeds that do not excite the tyre to a point that the tyre losses contact with the bump.

Figure 3-9(a) illustrates the APG bump test layout. Figure 3-9(b) illustrates the tests being conducted. The trailer (1) is accelerated from rest to a target speed of 10 km/h or 20 km/h before reaching the APG bump (2). The trailer speed is maintained constant by driving the towing vehicle (3) against the engine governor (Els, 2005). The speed is maintained constant as the trailer travels over the APG bump. Once the trailer has fully cleared the APG bump

© University of Pretoria

and the trailer has stabilised the tow vehicle is slowed down to a stop. An offset bar (4) is used to offset the tow hook on the tow vehicle such that the trailer goes over the APG bump and the tow vehicle does not go over the APG bump. This allows the tow vehicle to follow a straight path, so the vertical dynamic response of the trailer is isolated and not coupled with the dynamic lateral response of the towing vehicle.

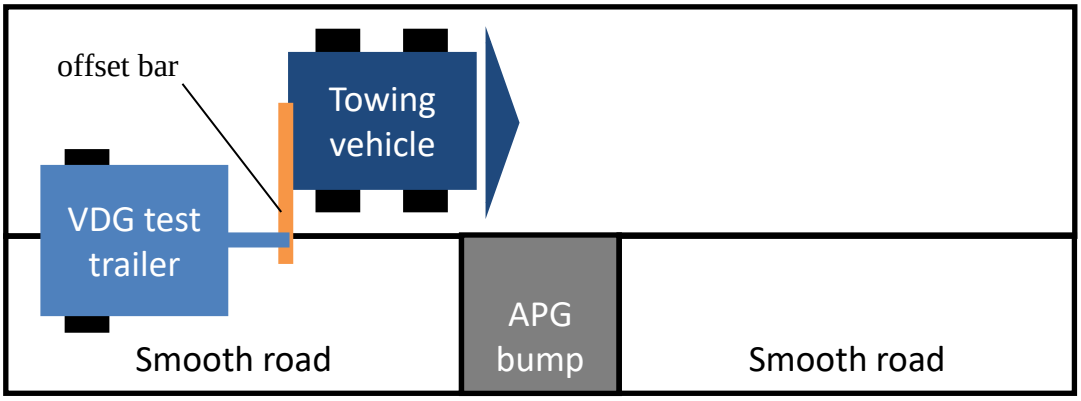

(a)

(b)

1	Trailer	**2**	APG bump
3	Towing vehicle	**4**	Offset bar

Figure 3-9 APG bump test layout (a) schematic (b) test setup

Figure 3-10 shows 4 points of interests when the tyre interacts with the APG bump. The 4 points of interest in Figure 3-10 correspond to the 4 labels in Figure 3-12, Figure 3-13 and Figure 3-14.

Point 1 corresponds to when the tyre makes contact with the APG bump. The suspension is compressed as the tyre moves up the ramp. Point 2 corresponds to when the tyre reaches the top of the APG bump. Point 3 corresponds to when the tyre rolls of the top of the APG bump.

© University of Pretoria

The suspension extends to keep the tyre in contact with the APG bump. Point 4 corresponds to when the tyre makes contact with the road after the bump.

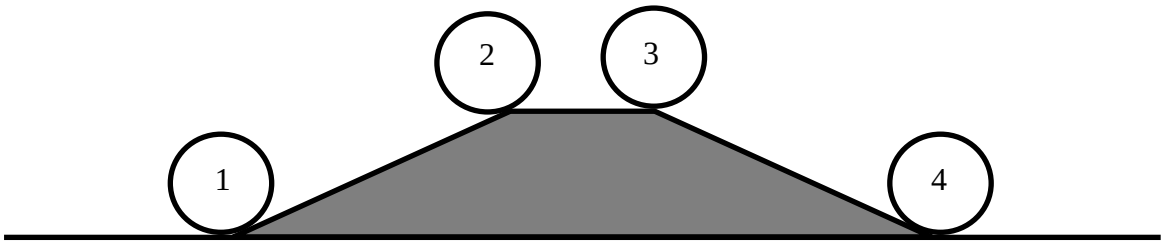

Figure 3-10 Points of interest in the APG bump test

For all tyre pressures the wheel experiences higher accelerations than the front and rear of the trailer. The reason is that the wheel is in direct contact with the bump and the front and rear of the trailer are separated from the bump by the suspension. The suspension absorbs some of the wheel's energy as the suspension is compressed and extended as the wheel rolls over the bump. Thus, less energy is transferred to the front and rear of the trailer.

Also, the trailer pitches about the tow hook as shown in Figure 3-11. The relationship between tangential acceleration and angular acceleration is given by Equation 3-2. The tangential acceleration (a) is described by the angular acceleration (α) and the radius (r). The subscripts R and F represent the rear and front respectively. The front and rear have the same angular acceleration about the tow hook. The front is closer to the tow hook. As a result of the front being closer to the tow hook than the rear, the rear experiences a higher vertical acceleration than the front.

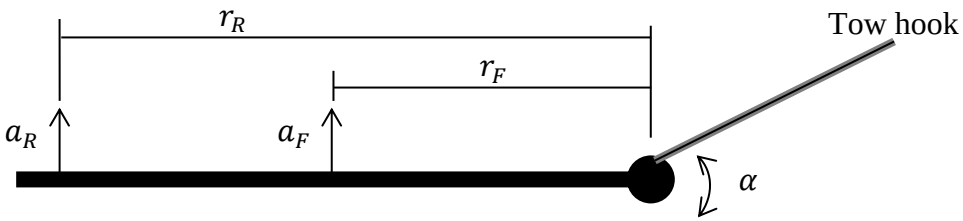

Figure 3-11 Trailer pitching

Equation 3-2

$$a = r\alpha$$

$$r_R > r_F$$

$$\therefore a_R > a_F$$

© University of Pretoria

Figure 3-12 to Figure 3-14 show the trailer test and simulation results recorded for the 100 mm APG bump traveling at 10 km/h with tyre pressures of 1.25 bar, 2.0 bar and 3.0 bar respectively. Parts (a), (b) and (c) in each figure respectively show that the wheel acceleration, rear acceleration and front acceleration simulation results, correlate well with the test results. Comparing test-1 and test-2 results it can be seen that the tests are precise and repeatable.

It can be seen that at 1.25 bar the wheel experiences a smoother acceleration, than the wheels at 2.0 bar and 3.0 bar. As the tyre pressure decreases, the tyre is able to deform more, thus dissipate more energy. As a result, a reduction in acceleration is experienced. Also at 1.25 bar, it is easier to distinguish when the tyre makes initial contact with the APG bump and when the tyre makes full contact with the APG bump, than at 2.0 bar and 3.0 bar. This is due to the tyre at 1.25 bar deforming more than the tyre at 2.0 bar and 3.0 bar. As a result, the delay between the tyre making initial contact and full contact with the AGP bump is longer for the tyre at 1.25 bar. In addition, at 2.0 bar and 3.0 bar it is easier to distinguish when the tyre reaches the top of the APG bump and rolls of the top of the APG bump, than at 1.25 bar. Again, this is due to the tyre at 1.25 bar deforming more than the tyres at 2.0 bar and 3.0 bar. Thus, the tyre enveloping effect at 1.25 bar is significantly more than at 2.0 bar and 3.0 bar.

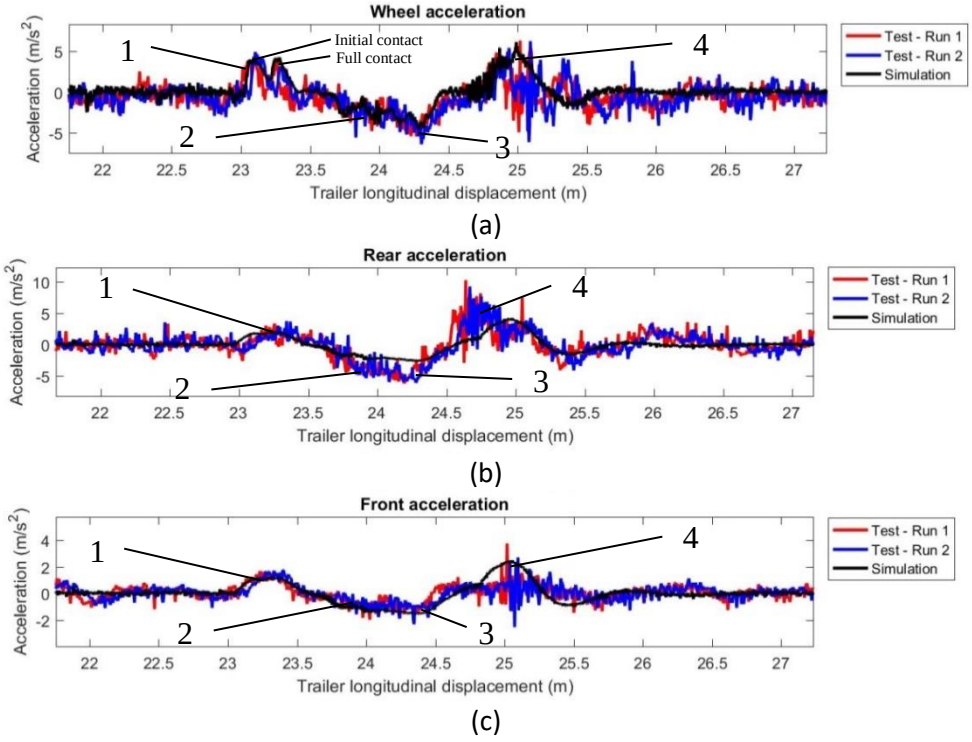

Figure 3-12 100 mm APG bump test at a tyre pressure of 1.25 bar traveling at 10km/h (a) wheel acceleration (b) rear acceleration (c) front acceleration

© University of Pretoria

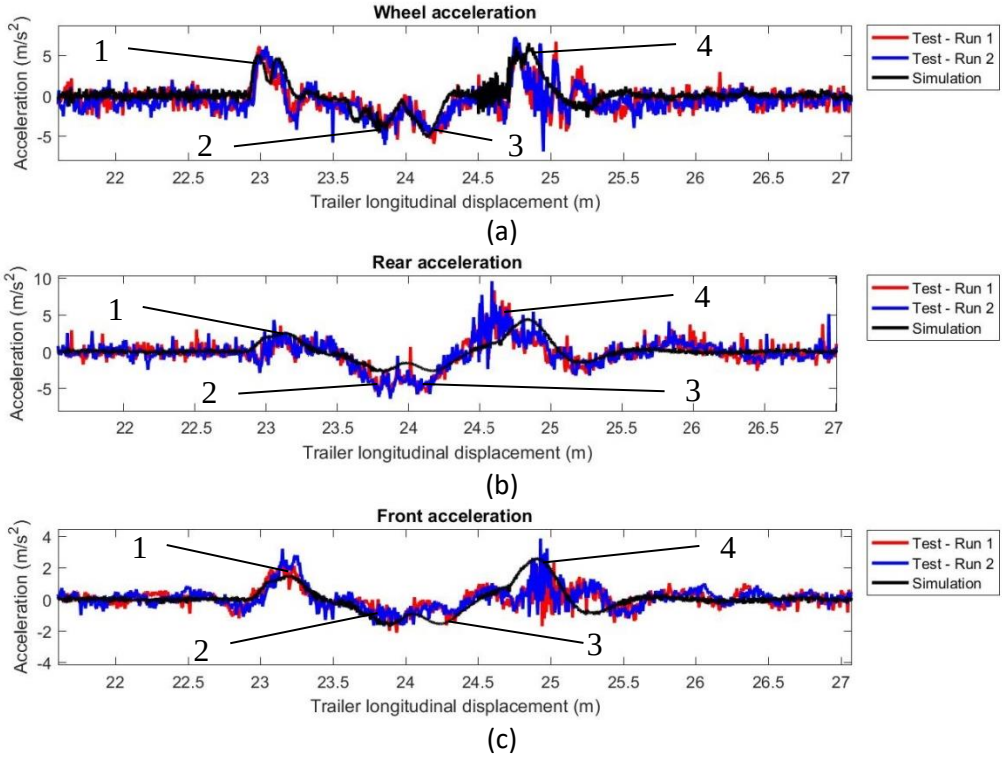

Figure 3-13 100 mm APG bump test at a tyre pressure of 2.0 bar traveling at 10km/h (a) wheel acceleration (b) rear acceleration (c) front acceleration

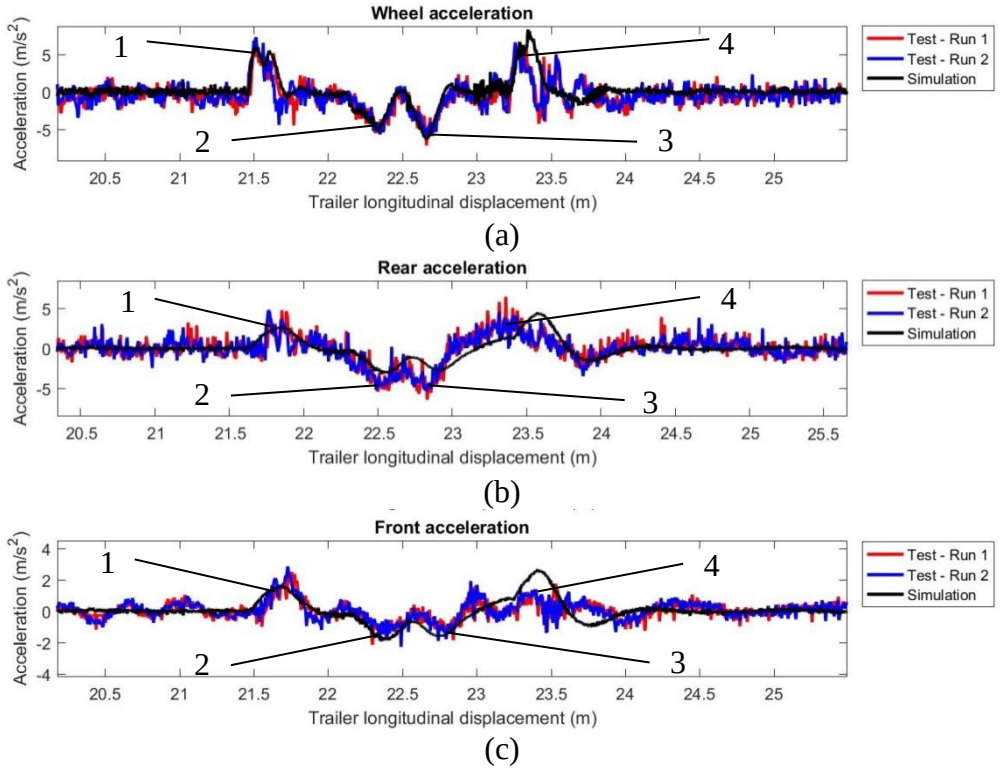

Figure 3-14 100 mm APG bump test at a tyre pressure of 3.0 bar traveling at 10km/h (a) wheel acceleration (b) rear acceleration (c) front acceleration

© University of Pretoria

Figure 3-15 to Figure 3-18 show the simulations of the trailer's right wheel centre's vertical displacement as the trailer travels over the $50\,mm$, $100\,mm$ and $150\,mm$ APG bump at target speeds of $10\,km$/h and $20\,km/h$.

When a tyre encounters a discrete obstacle, the tyre's contact patch wraps itself around the discrete obstacle. The tyre deforms around the discrete obstacle. Decreasing the tyre pressure increases the contact patch and increases the tyre's ability to deform. As a result, at lower tyre pressure the tyre is able to swallow a discrete obstacle and retain contact with the road.

Decreasing the tyre pressure increases the contact patch length of the tyre. An increase in the contact patch length due to a decrease in tyre pressure results in the tyre at $1.25\,bar$ making contact with the APG bump before the tyres at $2.0\,bar$ and $3.0\,bar$. It can be seen that the vertical wheel displacement of the tyre at $1.25\,bar$ increases first when approaching the APG bump. Also, once the APG bump is cleared, the $1.25\,bar$ tyre makes full contact with the road last. Thus, decreasing the tyre pressure adds a delay to the wheel's vertical displacement over a discrete obstacle.

The lagging delay is greater than the leading delay. The wheel's vertical displacement as the trailer travels over the APG bump can be divided into 2 sections, namely; leading the APG bump and lagging the APG bump. Leading the APG bump refers to the portion between the tyre making contact with the APG bump and the tyre reaching the top of the APG bump. At the top of the bump the tyre returns to its relaxing height. That is, the tyre deformation is only due to the loading and tyre pressure, not due to road irregularities. Lagging the APG bump refers to the portion between the top of the APG bump and the tyre making full contact with the road again.

Figure 3-15 shows the wheel's vertical displacement as the trailer travels over the $50\,mm$ APG bump at $10\,km/h$. Decreasing the tyre pressure increases the tyre enveloping effect. The tyre filters out more road irregularities as the tyre pressure decreases. The tyre enveloping effect is more beneficial over harsh road irregularities. The $50\,mm$ APG bump is a harsh steep APG bump in comparison to the $100\,mm$ APG bump and $150\,mm$ APG bump. It can be seen that the improvement in the vertical displacement smoothing is due to a decrease in tyre pressure, the improvement is more pronounced over the harsher $50\,mm$ APG bump than on the $100\,mm$ APG bump and $150\,mm$ APG bump. Only the tyre at $1.25\,bar$ is

© University of Pretoria

able to deform sufficiently to envelope over the harsh road input. At a tyre pressure of 2.0 bar and 3.0 bar the harsh road input makes the wheel jump.

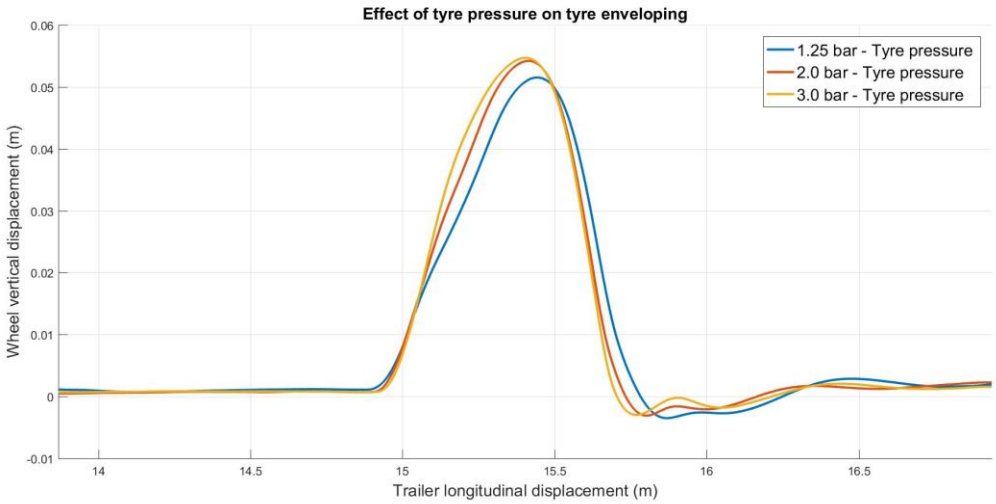

Figure 3-15 Effect of tyre pressure on tyre enveloping over a 50mm APG bump at 10 km/h

Figure 3-16 shows the wheel vertical displacement over a 100 mm APG bump at 10 km/h. It can be seen that decreasing the tyre pressure increases the tyre enveloping over the bump. As a result the wheel height is smoother over the APG bump at 1.25 bar than at 2.0 bar or 3.0 bar. It can be seen that as the tyre reaches the top of the APG bump at 2.0 bar or 3.0 bar, the wheel's vertical displacement abruptly flattens out. Conversely, the tyre at 1.25 bar continues to deform and deflect at the top of the APG bump. As a result, the wheel vertical displacement over the APG bump is smoother.

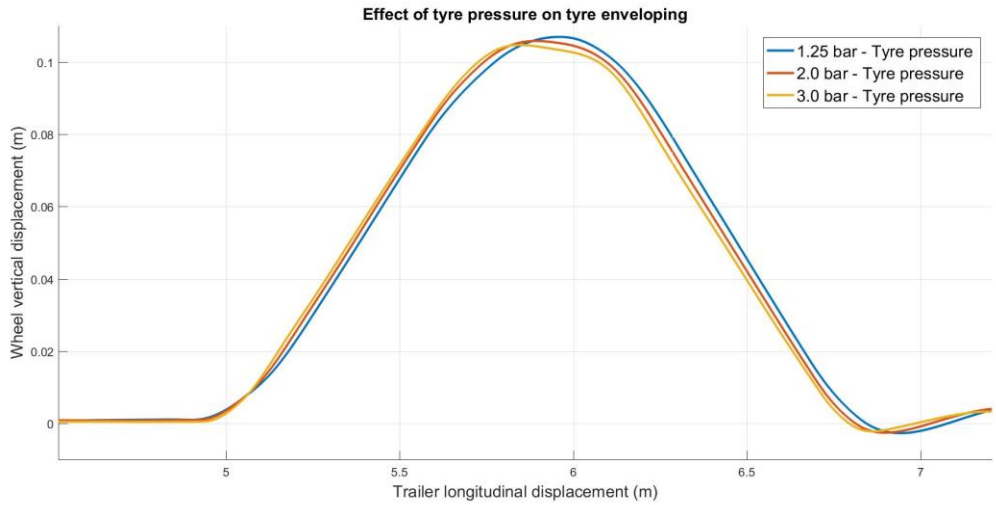

Figure 3-16 Effect of tyre pressure on tyre enveloping over a 100mm APG bump at 10 km/h

Figure 3-17 shows the wheel vertical displacement over a 150 mm APG bump at 10 km/h. The 150 mm APG bump is slightly more steep than the 100 mm APG bump, but at a speed

© University of Pretoria

of 10 km/h does not make the road input significantly more harsh. Therefore, the tyre enveloping affect is not significantly more on the 150 mm APG bump than on the 100 mm APG bump. The tyre response on the 150 mm APG bump is similar to its response on the 100 mm APG bump.

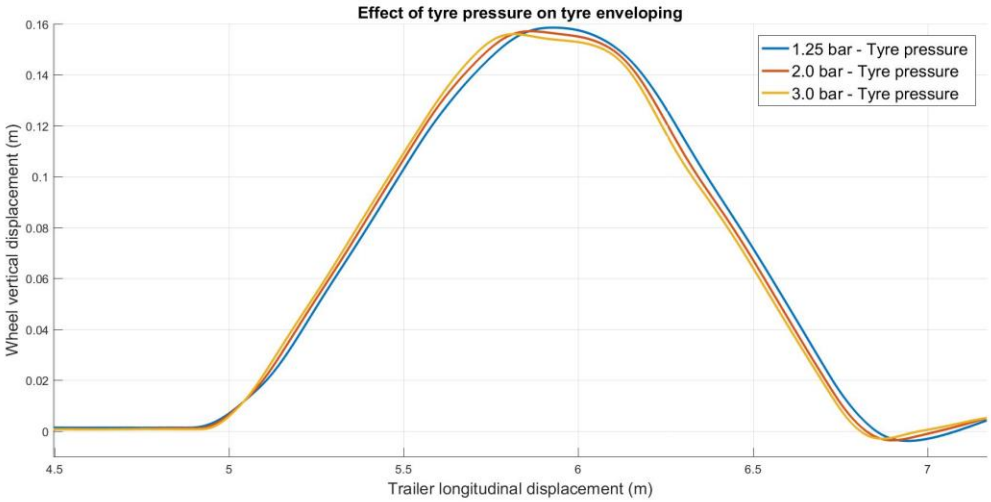

Figure 3-17 Effect of tyre pressure on tyre enveloping over a 150mm APG bump at 10 km/h

Figure 3-18 shows the wheel vertical displacement over a 100 mm APG bump at 20 km/h. Increasing the speed to 20 km/h over the 100 mm APG bump results in a harsher road input to the tyre. Again, the tyre enveloping effect is more evident as the road input becomes harsher. It can be seen that decreasing the tyre pressure allows the tyre to deform more. As a result, decreasing the tyre pressure leads to a smoothing out of harsh road inputs.

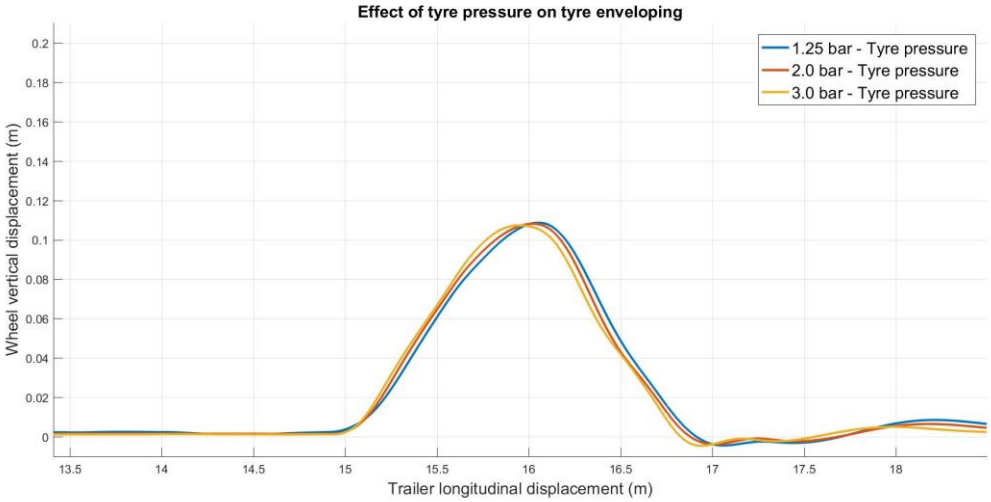

Figure 3-18 Effect of tyre pressure on tyre enveloping over a 100mm APG bump at 20 km/h

© University of Pretoria

3.2.3.3 Belgian paving validation tests

A further 6 Belgian paving tests were conducted at the Gerotek Test Facilities west of Pretoria, South Africa (Gerotek, 2020), to validate that the trailer model accurately estimates the behaviour of the actual trailer on rough roads. Figure 3-19 illustrates the Belgian paving test layout. The trailer is accelerated from rest to a target speed of $20km/h$, $40km/h$ and $60\ km/h$ on the smooth road before reaching the Belgian paving. Again, the trailer speed is maintained constant by driving the towing vehicle against the engine governor. Again, an offset bar is used so that only the trailer right wheel travels over the Belgian paving. Once the trailer fully clears the Belgian paving and returns back to the smooth road, the tow vehicle is slowed down to a stop.

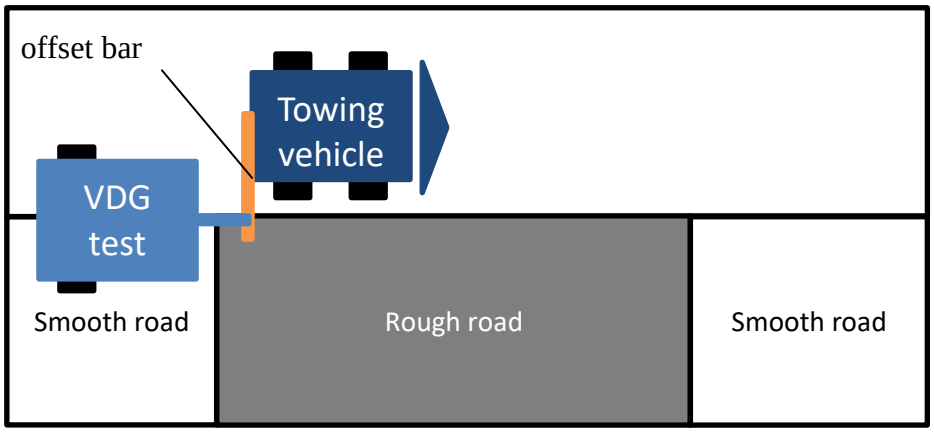

Figure 3-19 Rough road test layout

The Belgian paving gives random acceleration inputs to the trailer. A small change in the path of the trailer changes the acceleration inputs to the trailer rendering the acceleration results incomparable in the time domain. To overcome this, statistical analysis is used to analyse the Belgian paving results. Normal distribution is a useful comparison for datasets that are random in nature. The normal distribution of the acceleration test results makes the results meaningful. Each bin of the acceleration normal distribution is a count of the number of times the signal value is recorded in the sample.

The normal distribution characteristics can be seen from Figure 3-20 that 68% is within 1 standard deviation from the mean. 95% of the data is within 2 standard deviation from the mean. 99.7% of the data is within 3 standard deviations from the mean. Also, the distribution is symmetrical around the mean.

© University of Pretoria

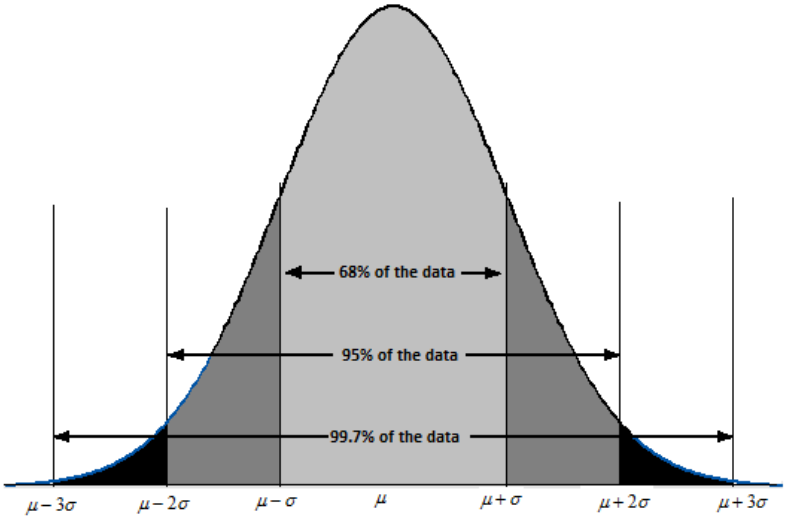

Figure 3-20 Normal distribution probability density function (Chegg, 2019)

To validate the trailer model on the rough road the wheel acceleration and rear acceleration from the test measurements are compared to those from the simulation measurements. Figure 3-21 shows the acceleration distribution of the test results and simulation results. Firstly, it can be seen that the tests are repeatable, because 'test-1' and 'test-2' acceleration distributions are comparable. Secondly, the trailer model accurately estimates the behaviour of the actual trailer, because the simulation and test acceleration distributions are comparable.

To quantify the correlation between the test results and simulation results, the mean error and standard deviation relative error are calculated using Equation 3-3 and Equation 3-4, respectively, where $x_{simulation}$ represents the mean or standard deviation of the simulation and x_{test} represents the mean or standard deviation of the test results. The mean relative error is not meaningful, because the mean is approximately zero.

Equation 3-3

$$error = |x_{test} - x_{simulation}|$$

Equation 3-4

$$R.E.\% = \left|\frac{x_{test} - x_{simulation}}{x_{test}}\right| \times 100\%$$

The acceleration distribution of the trailer model and the results are comparable. The errors between the normal distribution characteristic of the simulated trailer model and the test results are calculated and summarised in Table 3-6.

Figure 3-21(a) shows the wheel acceleration distribution and Figure 3-21(b) shows the rear acceleration distribution. The wheel acceleration maximum mean error is 0.01, and the

© University of Pretoria

maximum standard deviation relative error is 2.26%.The rear acceleration maximum mean error is 2.0×10^{-3}, and the maximum standard deviation relative error is 18.15%.

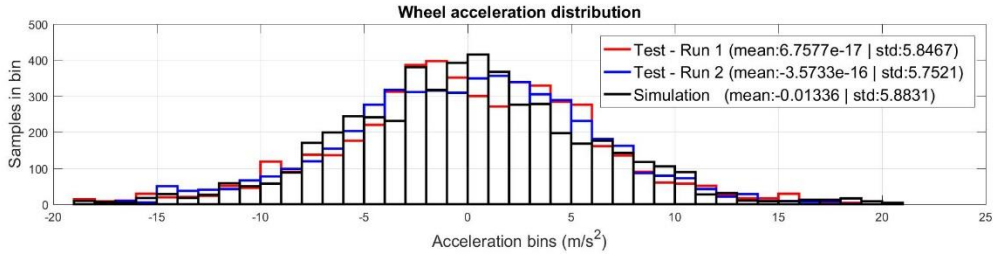

(a)

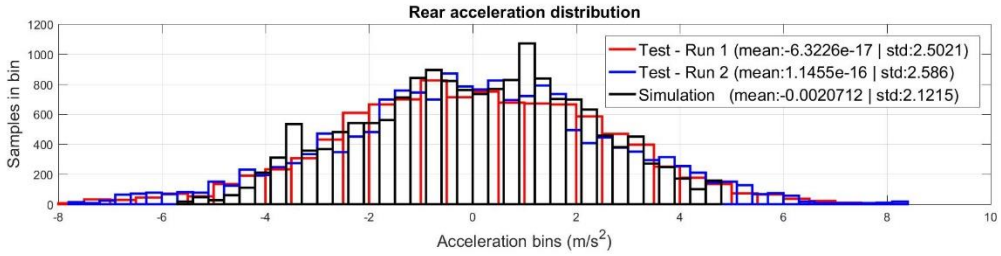

(b)

Figure 3-21 (a) Wheel acceleration distribution and (b) rear acceleration distribution at a tyre pressure of $1.0\ bar$ traveling at 60 km/h

Table 3-6 Mean absolute error and standard deviation relative error of the wheel acceleration and rear acceleration at 60 km/h

Tyre pressure		1.0 bar		2.0 bar		3.0 bar	
Acceleration		Mean	Standard deviation	Mean	Standard deviation	Mean	Standard deviation
Wheel	Simulation	1,30E-02	5,88	3,47E-03	8,42	2,59E-02	9,73
	Test – 1	6,76E-17	5,85	2,78E-16	8,38	1,14E-16	9,52
	Test – 2	3,57E-16	5,75	4,19E-16	8	4,08E-17	9,35
	Error – 1	0,013	0,51	0,00347	0,47	0,0259	2,20
	Error - 2	0,013	2,26	0,00347	5,25	0,0259	4,06
Rear	Simulation	2,07E-03	2,12	4,82E-03	2,38	6,75E-03	2,44
	Test – 1	6,32E-17	2,5	5,39E-17	2,92	1,35E-16	3,24
	Test – 2	1,15E-16	2,59	4,62E-17	2,78	2,00E-18	3,11
	Error – 1	0,00207	15,2	0,00482	18,49	6,75E-03	24,7
	Error - 2	0,00207	18,14	0,00482	14,38	6,75E-03	21,5

© University of Pretoria

3.3 Conclusion

The trailer model is validated and proves to be an accurate and reliable model. Three different tests were conducted to parametrise and validate the trailer model, namely; pneumatic system parametrisation tests, APG bump tests and Belgian paving tests.

The pneumatic system parametrisation test show that the tyre can be inflated from 1.0 bar to 3.0 bar in 8 s. The tyre can be deflated from 3.0 bar to 1.0bar in 13 s.

The APG bump tests were conducted to validate the body model and tyre model. The simulation results correlate with the test results. Therefore, the trailer model can be used over discrete obstacle (e.g. speed bumps, potholes and curbs) simulations. Decreasing the tyre pressure increases the tyre enveloping effect, thus smoothing out the road inputs. Decreasing the tyre pressure increases the ability of the tyre to absorb and dissipate unwanted road irregularities. Thus, less wheel accelerations will be transferred to the vehicle occupants, which will lead to an improvement in ride comfort.

Belgian paving tests were conducted to validate the body model and tyre model over rough roads. The simulation results correlate with the test results. Therefore, the trailer model can be used for rough road simulations. Both the wheel acceleration and rear acceleration mean is approximately zero. The wheel acceleration has a maximum standard deviation relative error of 5.25%, whereas, the rear acceleration has a maximum standard deviation relative error of 24.7%.

The trailer model closely approximates the behaviour of the actual trailer. Therefore, the TIPc can be designed based on this trailer model. There is confidence that a TIPc that improves the ride comfort of the trailer model on rough road simulations will also improve the ride comfort of the actual trailer on rough roads. The rear experiences high acceleration magnitudes than the front, consequently the rear experiences more discomfort than the front. So, the rear acceleration will be used as an indicator of discomfort for the TIPc.

© University of Pretoria

This page is intentionally left blank

© University of Pretoria

This page is intentionally left blank

© University of Pretoria

4 TIPc development and implementation

This chapter discusses the TIPc development and the implementation of the TIPc on the trailer.

Section 4.1 discusses the TIPc development in Simulink and MATLAB. The TIPc uses the rear acceleration to calculate two acceleration rms'. A long sampling distance acceleration rms is used to evaluate the ride comfort level. Based on this acceleration rms, the TIPc determines a suitable tyre pressure. A short sampling distance acceleration rms is used to prevent the TIPc from deflating the tyre due to a discrete obstacle.

Section 4.2 evaluates the implemented TIPc performance. The developed TIPc is programmed into a Diamond Systems Helios single board computer with analogue and digital IO, and implemented to the test trailer The ride comfort level of the pressure controlled tyre and passive tyre at 3.0 bar are compared to evaluate the benefit of a pressure controlled tyre.

4.1 TIPc development

The objective of the TIPc is to ensure that the ride comfort level is kept in the *NOT uncomfortable* region. Figure 4-1 shows how the TIPc relates the tyre pressure to the ride comfort level. If the ride comfort level is above *NOT uncomfortable* the tyre pressure is decreased to improve the vehicle ride comfort. If the ride comfort level is *NOT uncomfortable* the tyre pressure is maintained at the normal driving pressure of 3.0 bar. If the ride comfort level is between *A LITTLE uncomfortable* and *uncomfortable* the tyre is deflated to 2.0 bar. If the ride comfort level is either *VERY uncomfortable* or *EXTREMELY uncomfortable* the tyre is deflated to 1.0 bar.

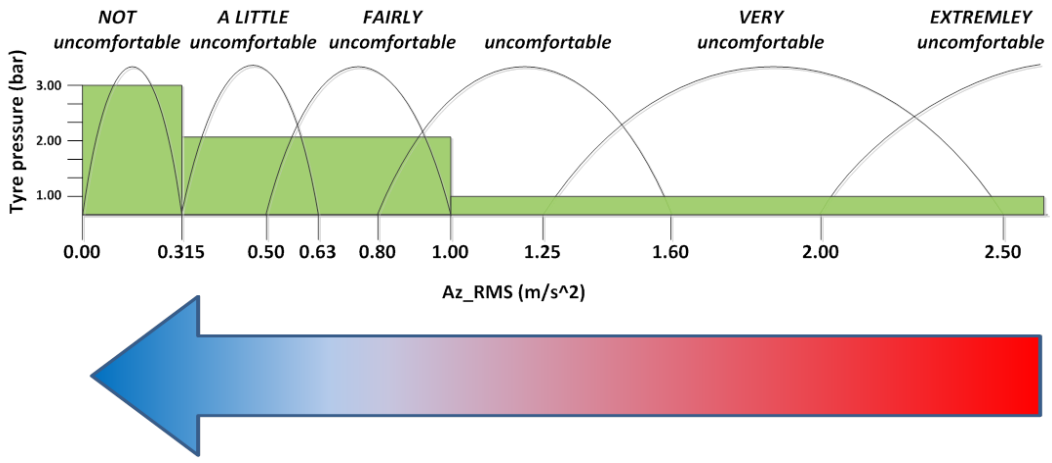

Figure 4-1 TIPc objective

© University of Pretoria

Figure 4-2 shows how the necessary TIPc equipment is connected together. The Helios functions as both the data recorder and TIPc. The rear acceleration is used to determine the ride comfort level. The TIPc determines a suitable tyre pressure depending on the ride comfort level. The TIPc then sends a signal to the MPPES to inflate or deflate the tyre to the selected tyre pressure. The tyre pressure transducer is used to ensure that the tyre is inflated or deflated to the selected tyre pressure. The tank pressure transducer is used to check if there is sufficient pressurised air to inflate the tyre and to prevent from deflating the tyre if there is not sufficient pressurised air in the tank to re-inflate the tyre to the normal driving tyre pressure.

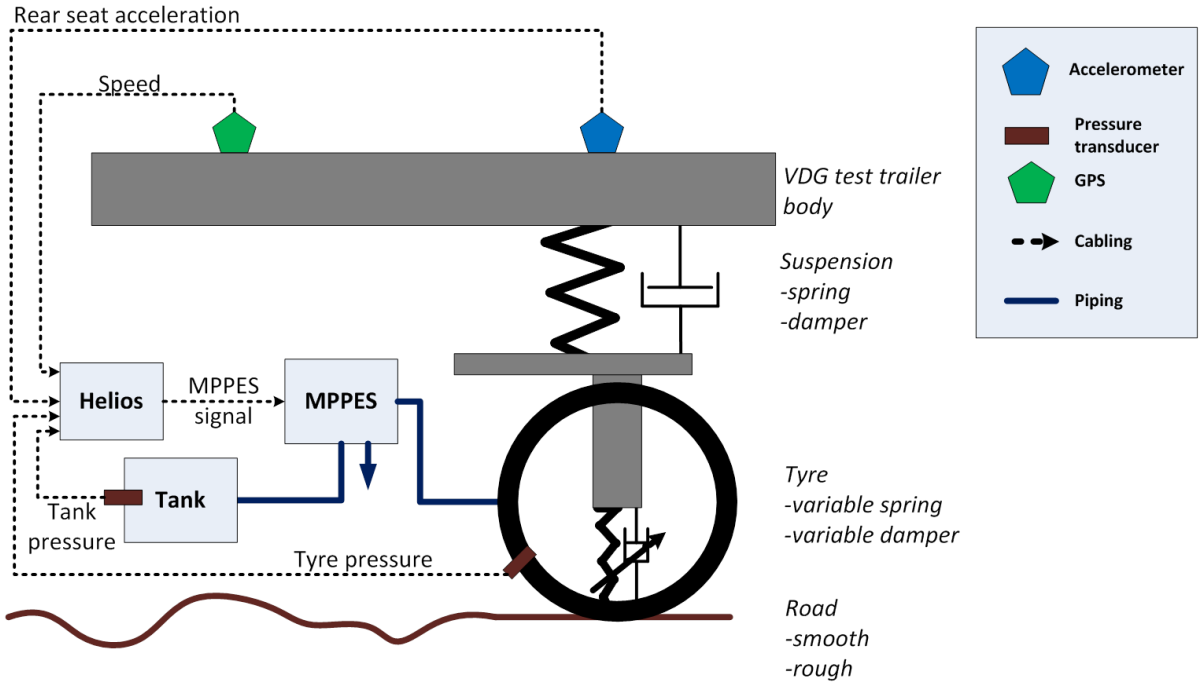

Figure 4-2 TIPc setup

At every time step two new rear acceleration rms'are calculated. The process followed to calculate acceleration rms' is shown in Figure 4-3, the steps are as follows:

1. The ride comfort evaluation begins with the measurement of the rear acceleration. The rear acceleration goes through a ring buffer to create a moving acceleration vector.
2. The acceleration vector in the time domain is transformed to the frequency domain.
3. The acceleration vector in the frequency domain is multiplied with the w_b weighting function (British Standards Institution 6841, 1987).
4. The weighted acceleration in the frequency domain is then transformed back to the time domain.

© University of Pretoria

5. Finally, the two rms' (long sampling distance rms and short sampling distance rms) for the w_b weighted acceleration in the time domain are calculated, which are discussed further in section 4.1.1 (Sampling distance sensitivity study).

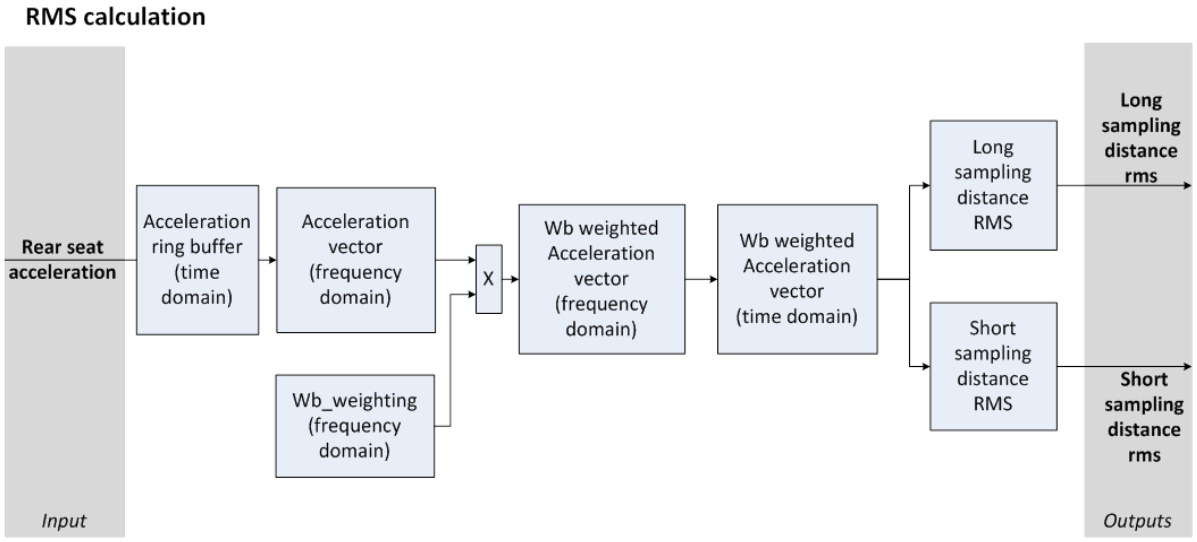

Figure 4-3 Ride comfort evaluation

The acceleration rms is calculated using Equation 4-1, where a_n is the w_b weighted acceleration vector and N is the number of points. RMS is a statistical measure of the mean of data with positive and negative values, as the method weighs each value as positive. (Park & Subramaniyam, 2013).

Equation 4-1

$$a_{rms} = \sqrt{\frac{1}{N}\sum_{n=1}^{N} {a_n}^2}$$

$$\lim_{N \to 1} a_{rms} = \sqrt{\frac{1}{N}\sum_{n=1}^{N} {a_n}^2} = a_n$$

Two observations are made from Equation 4-1

i. The limit of N approaching 1, a_{rms} goes to $|a_n|$. So, using a few sampling points cannot be used to determine the rms.

© University of Pretoria

ii. The limit of N approaching ∞, a_{rms} goes to the statistically stationary mean. So, using too many sampling points cannot be used to identify the change from a smooth road to a rough road.

4.1.1 Sampling distance sensitivity study

A sampling distance sensitivity study was conducted to determine the most suitable sampling distance that the TIPc must use to evaluate the ride comfort. Two considerations when determining the most suitable sampling distance are; the acceleration vector length must be long enough that the TIPc can calculate a moving rms accurately to evaluate the ride comfort and the acceleration vector must not be too long and introduce excessive delays to the calculated rms. Increasing the number of sampling points improves the TIPc accuracy at the cost of computing speed.

The number of points used to calculate the acceleration rms is determined by Equation 4-2. The number of sampling points (N) is described by speed (v), sampling frequency (SF) and sampling distance (SD). A trade-off between the sampling distance and the sampling frequency is required to ensure the Helios has sufficient computing power to perform the calculations within the sampling frequency.

Equation 4-2

$$N = \frac{3.6(km \cdot s/m \cdot h)}{v(km/h)} \times SF(points/s) \times SD(m)$$

Belgian paving and a $100\,mm$ APG bump were used to evaluate the ride comfort level sensitivity to the sampling distance on rough roads and discrete obstacle (e.g. speed bumps, potholes and curbs) respectively. The trailer is accelerated from rest to a target speed of $50\ km/h$ on a smooth road. From the smooth road the trailer travels over the Belgian paving. Then back to the smooth road. Finally, the trailer goes over an APG bump. The trailer speed is maintained constant throughout the simulation.

Figure 4-4 shows the rear acceleration rms sensitivity to sampling distance when traveling at $50\ km/h$. It can be seen that calculating the acceleration rms with a sampling distance of $0.5m$ results in a volatile acceleration rms. A short sampling distance does not accurately calculate the ride comfort level. Calculating the rms with a sampling distance of $35\ m$ results in a delayed acceleration rms response. The rms peaks and remains high long after the discrete obstacle is actually cleared. A long sampling distance gives the impression the trailer

© University of Pretoria

is traveling on a rough road when actually traveling over a discrete obstacle. A long sampling distance rms cannot differentiate between an uneven road and a discrete obstacle.

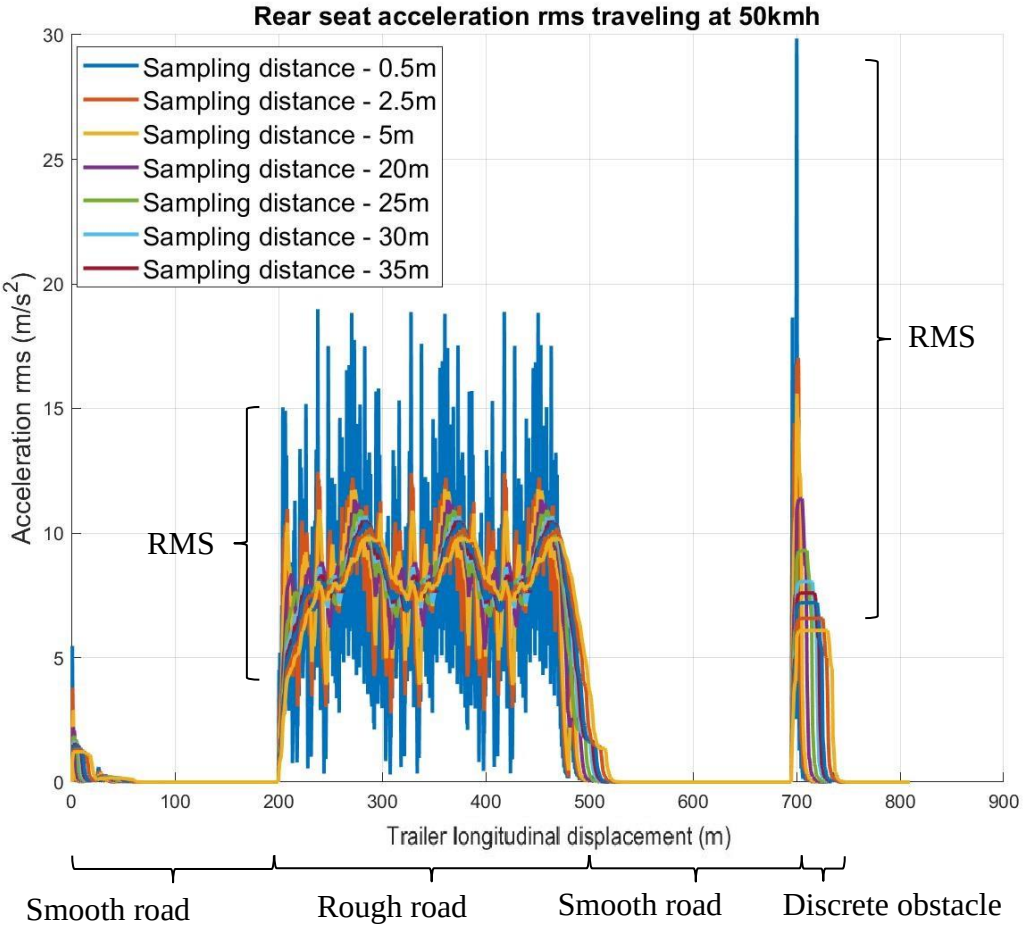

Figure 4-4 Sampling distance vs RMS sensitivity at 50 km/h

Figure 4-5 shows the RMSo (RMS overshoot) for the trailer changing terrain from a smooth road to a rough road and traveling over a discrete obstacle. The RMSo is defined as the absolute difference of a long sampling distance rms (rms_{long}) and a short sampling distance rms (rms_{short}) as shown in Equation 4-3. The long sampling distance is selected to be $25m$ and the short sampling distance is 15% of the long sampling distance. It can be seen that when travelling on the smooth road the RMSo is close to zero. When the trailer changes terrain to the rough the RMSo fluctuates between 0-7 m/s^2. When the trailer goes over the APG bump the RMSo peaks above 9. The RMSo when the trailer travels over a discrete obstacle is greater than the peak when traveling on the rough road. Thus, the RMSo can be used to detect discrete obstacles. The RMSo can differentiate between a discrete obstacle and a change in terrain from a smooth road to a rough road. When the RMSo is above a threshold

© University of Pretoria

of $5m/s^2$, theTIPc identifies that the increase in acceleration rms is due to a discrete obstacle and the TIPc does not change the tyre pressure. When the RMSo is below a threshold the TIPc identifies that the increase in rms is due to a change in terrain and the TIPc determines a suitable tyre pressure for the road condition.

Equation 4-3

$$RMSo = \left|rms_{long} - rms_{short}\right|$$

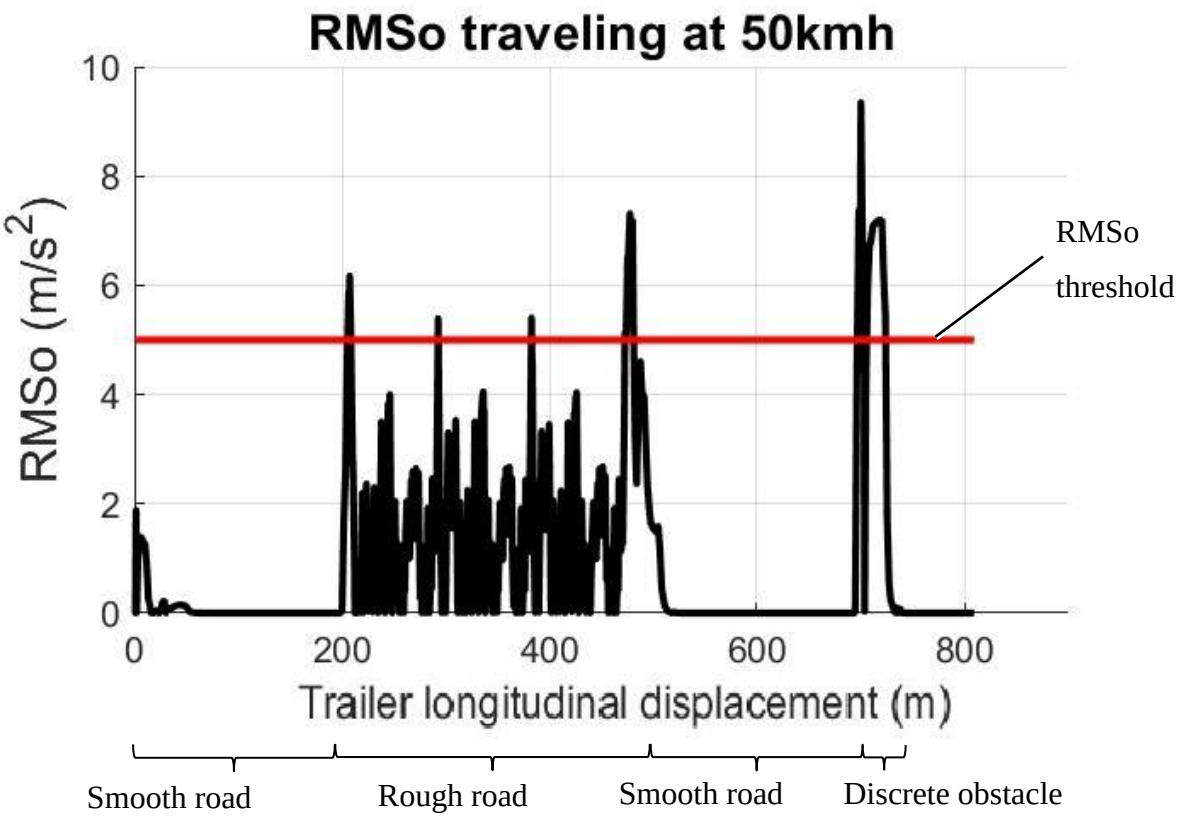

Figure 4-5 RMS overshoot

4.1.2 TIPc logic

Figure 4-6 illustrates the control logic followed by the TIPc. The steps are as follows:

1. Continuing from the rms' (long sampling distance rms and short sampling distance rms) calculated in Figure 4-3, the RMSo is calculated. If the RMSo is less than the RMSo threshold, then the TIPc proceeds to the next step.
2. The speed is integrated to determine the distance travelled. If the difference between the distance travelled and the location of the previous tyre pressure change is greater than the sampling distance, then the TIPc proceeds to the next step.

© University of Pretoria

3. Based on the long sampling distance rms the TIPc determines a suitable tyre pressure. If the ride is *NOT uncomfortable* the tyre pressure is set to 3.0 bar. If the ride is A *LITTLE uncomfortable* or *FAIRLY uncomfortable* the tyre pressure is set to 2.0 bar. Otherwise, the tyre pressure is set to 1.0 bar.
4. Before the selected tyre pressure signal is sent to the MPPES, the TIPc checks if there is sufficient pressurised gas in the tank to re-inflated the tyre to the normal driving pressure if the vehicle changes to a smooth road.
5. If the new tyre pressure is greater than the current tyre pressure the TIPc sends a deflate signal to the MPPES. If the new tyre pressure is less than the current tyre pressure the TIPc sends an inflate signal to the MPPES. The last inflation location is updated to the current location.

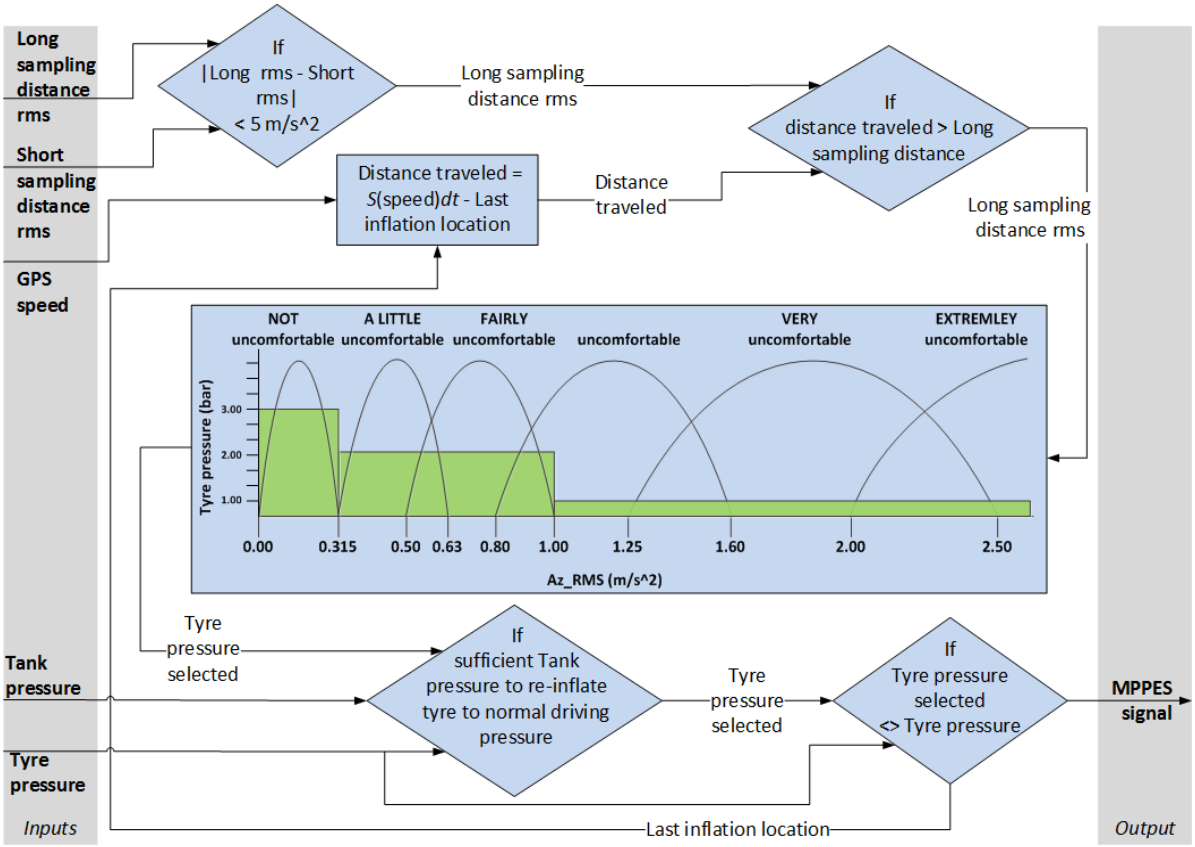

Figure 4-6 TIPc control logic

The TIPc model was added to the trailer model to evaluate the RCI (Ride Comfort Improvement) a pressure controlled tyre can achieve. Three tyre conditions are investigated; passive tyre at 1.0 bar, passive tyre at 3.0 bar and a pressure controlled tyre. The pressure controlled tyre acceleration rms is compared to the acceleration rms of a passive tyre at 3.0 bar (the normal driving pressure). Firstly, the trailer is accelerated from rest to a target

© University of Pretoria

speed of $30\ km/h$ and $40\ km/h$ on the smooth road. Then, the trailer travels on a rough road. After the rough road, the trailer returns to a smooth road. Finally, the trailer goes over a discrete obstacle.

To evaluate the TIPc performance the RCI is calculated by Equation 4-4. RCI is described by the acceleration rms for the passive tyre at $3.0\ bar(rms_{Passive\ at\ 3bar})$ and by the acceleration rms of the pressure controlled tyre ($rms_{Pressure\ controlled}$).

Equation 4-4

$$RCI = \frac{rms_{Passive\ at\ 3bar} - rms_{Pressure\ controlled}}{rms_{Passive\ at\ 3bar}} \times 100\%$$

Figure 4-7 and Figure 4-8 shows that the TIPc can differentiate a discrete obstacle from a rough road at $30\ km/h$ and $40\ km/h$ respectively. When a change in terrain is detected (smooth road to rough road or rough road to smooth road) the TIPc determines the most suitable tyre pressure to improve ride comfort.

It can be seen in Figure 4-7(a) that initially when traveling on the smooth road, the acceleration rms is in the *NOT uncomfortable* region. As a result the tyre pressure is at $3.0\ bar$ as shown in Figure 4-7 (b). When the trailer changes to the rough road the ride comfort becomes *EXTEREMLY uncomfortable*. Because, the RMSo shown in Figure 4-7(c) is below the threshold, the TIPc classifies the change in ride comfort level as a result of a terrain change. The TIPc then deflates the tyre to $1.0\ bar$. As the pressure controlled tyre deflates, the acceleration rms decreases from the acceleration rms of the passive tyre at 3.0 bar to the acceleration rms of the passive tyre at 1.0 bar. As the pressure controlled tyre pressure decreases the RCI increases as shown in Figure 4-7(d). The RCI fluctuates between $0 - 45\%$ with a mean of 8.5%. When the trailer returns to the smooth road, the ride comfort level returns to *NOT uncomfortable,* as a result the pressure controlled tyre inflates to $3.0\ bar$. When the trailer goes over the APG bump, the TIPc identifies the change in ride comfort level due to a discrete obstacle. The RMSo exceeds the threshold, thus the TIPc does not deflate the tyre even though the ride comfort level is temporarily *EXTREMELY uncomfortable*.

© University of Pretoria

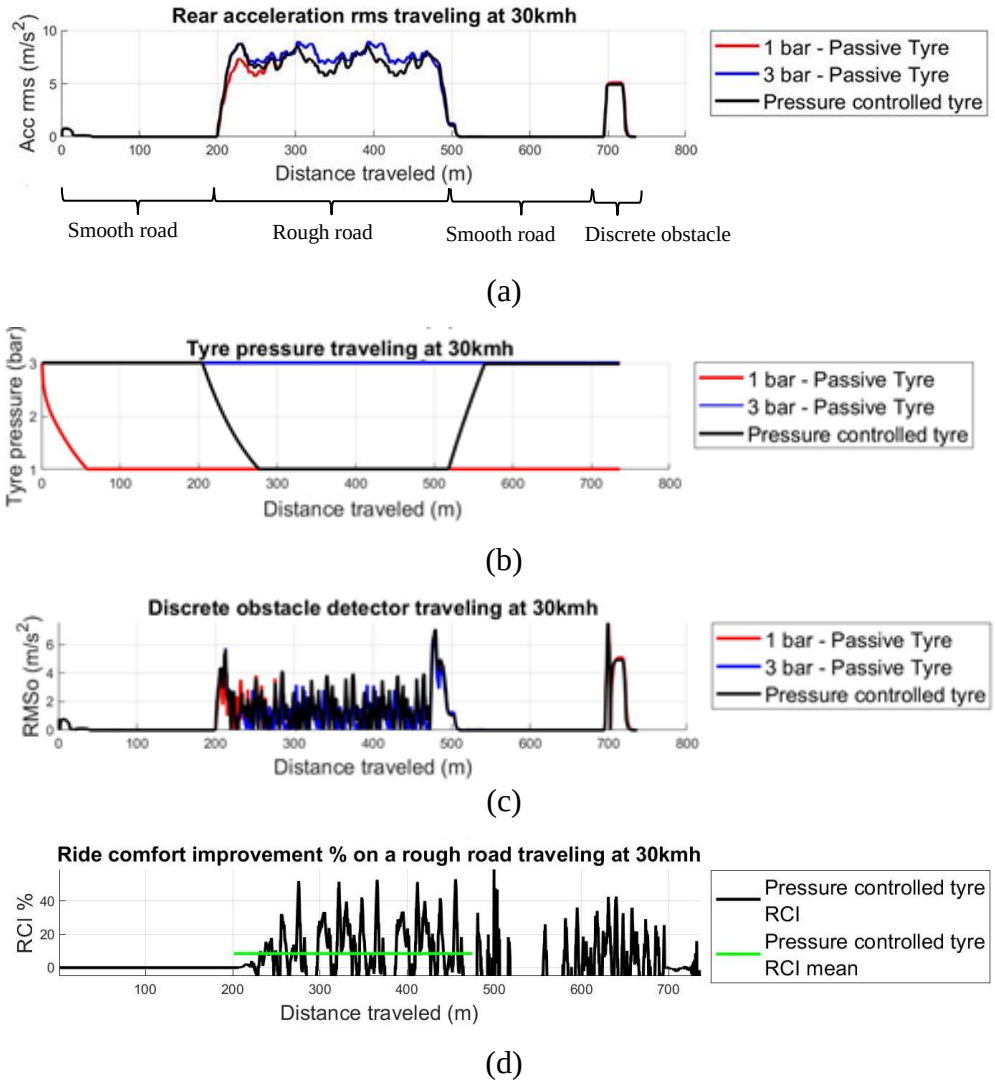

Figure 4-7 TIPc design performance traveling at 30 km/h (a) rear acceleration RMS (b) tyre pressure (c) RMSo (d) RCI

The TIPc responds similar when traveling at 40 km/h to when traveling at 30 km/h as shown in Figure 4-8. It can be seen in Figure 4-8(a) that initially when traveling on the smooth road the acceleration rms is in the *NOT uncomfortable* region, therefore the tyre pressure is at 3.0 bar as shown in Figure 4-8(b). When the trailer changes terrain to rough road the ride comfort becomes *EXTEREMLY uncomfortable*. Because, the RMSo shown in Figure 4-8(c) is below the threshold, the TIPc deflates the tyre to 1.0 bar. As the pressure controlled tyre deflates the acceleration rms decreases from the acceleration rms of the passive tyre at 3.0 bar to the acceleration rms of the passive tyre at 1.0 bar. As the pressure controlled tyre pressure decreases the RCI increases as shown in Figure 4-8(d). The RCI fluctuates between $0 - 45\%$ with a mean of 8.1%. When the trailer returns to the smooth road the ride comfort level return to *NOT uncomfortable*, as a result the pressure controlled tyre inflates to 3.0 bar. When the trailer goes over the APG bump, the TIPc identifies the

© University of Pretoria

change in ride comfort level is due to a discrete obstacle. The RMSo exceeds the threshold, thus the TIPc does not deflate the tyre even though the ride comfort level is temporarily *EXTREMELY uncomfortable*.

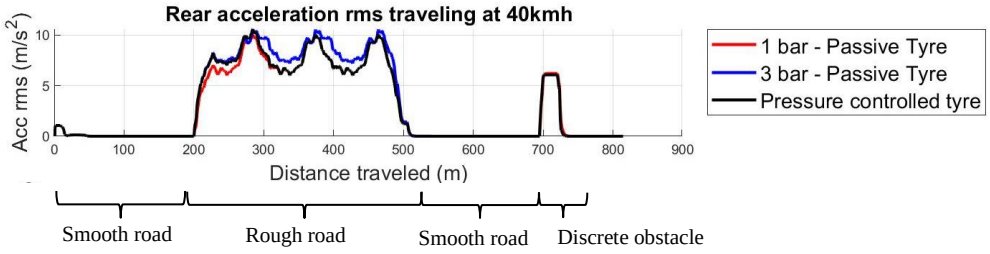

(a)

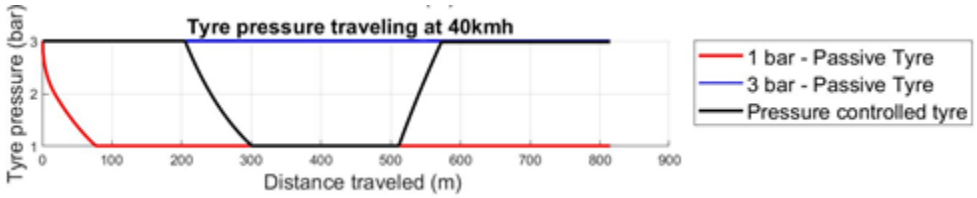

(b)

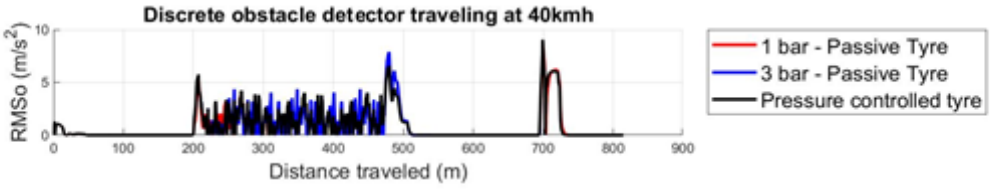

(c)

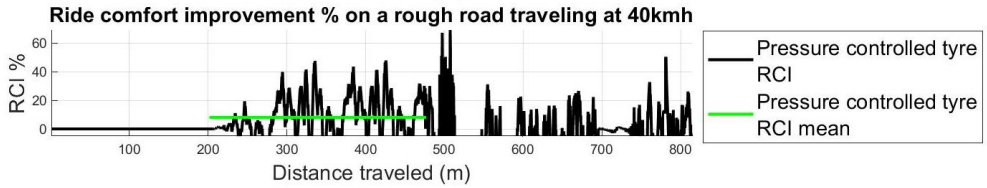

(d)

Figure 4-8 TIPc design performance traveling at 40 km/h (a) rear acceleration RMS (b) tyre pressure (c) RMSo (d) RCI

4.2 TIPc implementation and test results

The developed TIPc in Simulink and MATLAB was then converted to C++ code and implemented on the Helios. The TIPc implementation tests were conducted at the University of Pretoria's LC de Villiers Sportsground (GPS coordinates: -25.74462, 28.26086). Figure 4-9 shows the road layout were the tests were conducted. The tests begin and end on the paved road. The trailer is accelerated from stationary to a target speed of 30 km/h and 40 km/h. The target speed is maintained constant on parts of the road it is safe to do so, i.e. straight sections. The trailer speed is decreased to lower safe speeds when making a turn and

© University of Pretoria

the trailer speed is increased back to the target speed when it is once again safe to do so. From the paved road the trailer travels on the gravel road. From the gravel road the trailer changes terrain to the dirt road. Next the trailer changes terrain back to the paved road and the trailer is slowed down to a stop.

At each speed the tests were conducted for a passive tyre at 1.0 bar, passive tyre at 3.0 bar and a pressure controlled tyre. For each speed and tyre type the test was performed twice to ensure repeatability of results. Thus, a total of 12 tests were conducted. Unfortunately, the tyre pressure transducer became faulty when performing the passive tyre at $1.0\ bar$ and traveling at $30\ km/h$. Therefore, the passive tyre at $1.0\ bar$ and traveling at $30\ km/h$ results are omitted.

(a)

(b)

(c)

(d)

Figure 4-9 TIPc implementation tests (a) roads layout (b) paved road (c) dirt road (d) gravel road

Figure 4-10 and Figure 4-11 evaluates the performance of the implemented TIPc on the trailer. At all speeds the rear acceleration rms is highest when traveling on the gravel road and lowest on the paved road. It is difficult to distinguish between the gravel road and the dirt road by looking at the acceleration rms. This suggests that the road class for the gravel road and dirt road are close or even the same.

The trailer experienced low vertical accelerations from these roads, resulting in a low acceleration rms. The ride comfort level was *NOT uncomfortable* on the gravel road. By

© University of Pretoria

virtue of the ride comfort level not exceeding the *NOT uncomfortable* region, the TIPc parameters were lowered. When the acceleration rms is below $0.05\ m/s^2$ the tyre pressure is set to $3.0\ bar$ and when the acceleration rms in above $0.05\ m/s^2$ the tyre pressure is set to $1.0\ bar$. This is so that the tyre is deflated to $1.0\ bar$ on the gravel road and inflated to $3.0\ bar$ on the paved road. By so doing, the TIPc working principles can be illustrated.

The trailer was accelerated from rest to a target speed of $30\ km/h$ as shown in Figure 4-10(c). The acceleration rms increases as shown in Figure 4-10(a). When the trailer acceleration rms exceeds $0.05\ m/s^2$ the TIPc deflates the tyre to $1.0\ bar$ as shown in Figure 4-10(b). When the trailer returns to the paved road the acceleration rms decreases to below $0.05\ m/s^2$. As a result, the TIPc inflates the tyre to $3.0\ bar$. It can be seen that the pressure controlled tyre acceleration rms is less than the passive tyre at $3.0\ bar$ acceleration rms.

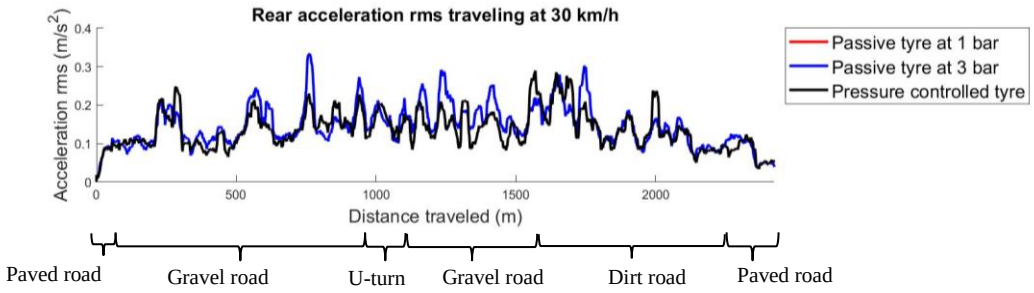

(a)

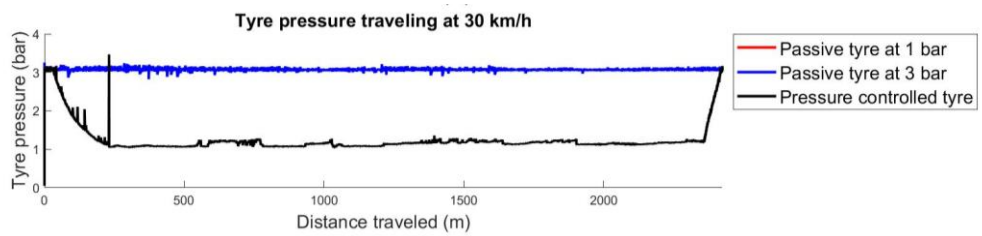

(b)

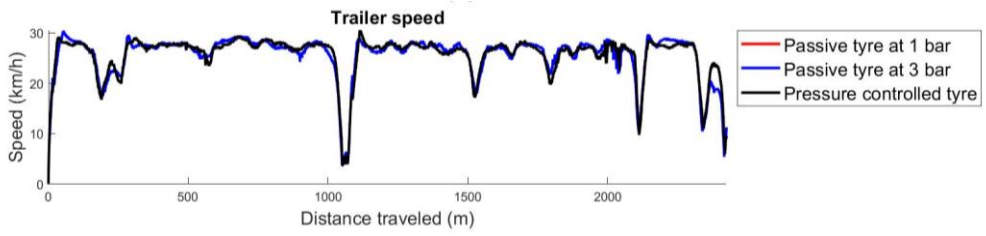

(c)

Figure 4-10 (a) TIPc implementation test traveling at target speed of $30\ km/h$ (a) rear acceleration rms (b) tyre pressure (c) actual speed

© University of Pretoria

The trailer was accelerated from rest to a target speed of $40\,km/h$ as shown in Figure 4-11(c). Increasing the trailer speed increases the acceleration rms experienced by the trailer, but the ride comfort level remains in the *NOT uncomfortable* region. When the trailer acceleration rms as shown in Figure 4-11 (a) exceeds $0.05\,m/s^2$, the TIPc deflates the tyre to $1.0\,bar$ as shown in Figure 4-11 (b). When the trailer returns to the paved road the acceleration rms decreases to below $0.05\,m/s^2$. As a result, the TIPc inflates the tyre to $3.0\,bar$. It can be seen that the pressure controlled tyre acceleration rms is less than the passive tyre at $3.0\,bar$ acceleration rms.

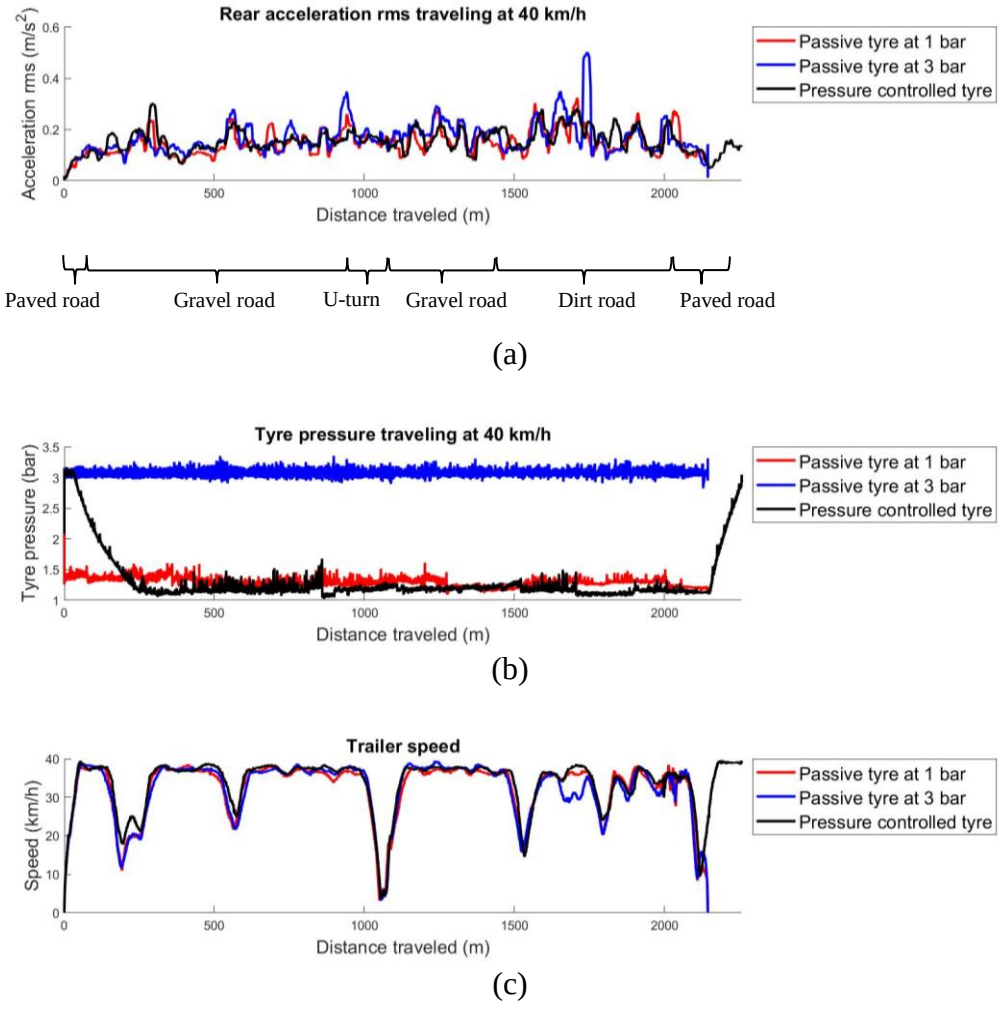

Figure 4-11 TIPc implementation test traveling at target speed of $40\,km/h$ (a) rear acceleration rms (b) tyre pressure (c) actual speed

Figure 4-12(a) and Figure 4-12(b) show the implemented TIPc performance traveling at $30\,km/h$ and $40\,km/h$, respectively. The moving acceleration rms shown in Figure 4-10 and Figure 4-11 cannot be used to quantify a moving RCI in the time domain. Hence, the overall RCI is used to quantify the TIPc performance. At $30\,km/h$ the TIPc achieves a 4%

© University of Pretoria

improvement in ride comfort. At 40 km/h the TIPc achieves a 7% improvement in ride comfort.

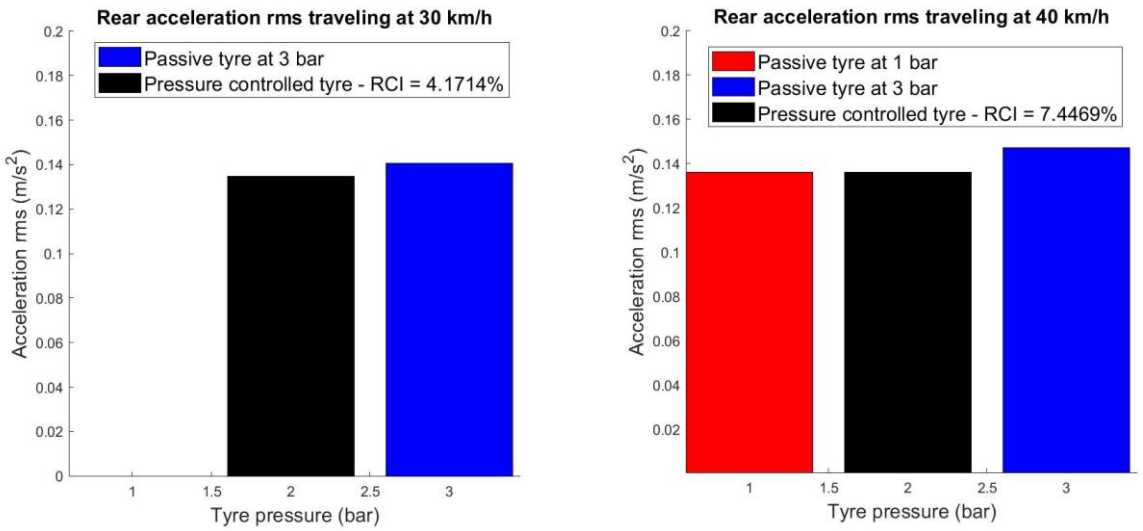

(a) (b)

Figure 4-12 TIPc implementation tests RCI traveling at (a) 30 km/h and (b) 40 km/h

4.3 Conclusion

The TIPc is designed to maintain the ride comfort level in the *NOT uncomfortable* level. To achieve this, the TIPc uses the rear acceleration to calculate two rms' namely: long sampling distance rms to determine the ride comfort level and a short sampling distance rms to detect discrete obstacles. RMSo accurately differentiates discrete obstacles from a rough road, thus the TIPc is robust.

Simulation results show that a mean of 8% improvement in ride comfort is achievable by a pressure controlled tyre on rough roads. Even though the pressure controlled tyre improves ride comfort, if the ride comfort level is in the *EXTREMELY uncomfortable* reducing the speed is also necessary to get the ride comfort level to the *NOT uncomfortable* region.

During the TIPc implementation tests the TIPc parameters were lowered, because the rear acceleration experienced by the trailer did not exceed the *NOT uncomfortable* region. The TIPc parameters were lowered, so that the TIPc is active and selects different tyre pressures when travelling on the gravel road and paved road to illustrate the working principles of the TIPc. Test results show that a pressure controlled tyre improves ride comfort on gravel roads by $4 - 7\%$.

© University of Pretoria

This page is intentionally left blank

© University of Pretoria

This page is intentionally left blank

© University of Pretoria

5 Conclusion

It has been identified that a pressure controlled tyre has the potential to improve ride comfort for passenger vehicles on rough roads. This study successfully developed a TIPc to improve ride comfort for passenger vehicles on rough roads.

To investigate the influence of tyre pressure on ride comfort a vehicle model with in-situ tyre inflation was created and validated against the actual trailer. Test results prove that the trailer model is an accurate and reliable representation of the actual trailer.

The validated model was used to develope the TIPc. The TIPc is designed to determine the most suitable tyre pressure depending on the ride comfort level, and deflate or inflate the tyre as required to maintain the ride comfort level *NOT uncomfortable*. The TIPc is robust on both smooth roads and rough roads and can detect bumps in the road.

Simulation of the TIPc implemented to the trailer model showed an improvement in the trailer ride comfort on rough roads. Simulation results show that the TIPc can improve ride comfort by 8% on Belgian paving. But, on rough roads such as Belgian paving, reducing the speed is necessary in conjunction with decreasing the tyre pressure to improve the ride comfort to the *NOT uncomfortable* region.

Having proven that the TIPc improves ride comfort through simulations, the TIPc was then implemented on the actual trailer. Test results of the TIPc implemented on the actual trailer also show an improvement in the ride comfort of the trailer. Test results prove the working principles and robustness of the TIPc. The TIPc achieved a $4.1 - 7.5\%$ improvement in ride comfort. It should be noted that the TIPc implementation tests were performed on paved road, dirt road and gravel road which are not as rough as the Belgian paving; therefore it is expected that the implemented TIPc would achieve a smaller improvement in ride comfort than the Belgian paving simulations.

© University of Pretoria

This page is intentionally left blank

© University of Pretoria

6 Recommendations

Several recommendations for future pressure controlled tyre investigations have been identified and are listed as follows:

- Add a speed controller to the TIPc. If the TIPc has deflated the tyre pressure to the lowest safe tyre pressure, but the ride comfort level remains above the *uncomfortable* ride comfort level, the TIPc must automatically reduce the vehicle speed to further improve the ride comfort level to the *NOT Uncomfortable* ride comfort level.
- The implemented TIPc performance must be evaluated experimentally on harsher road classes.
- Investigate on which road classes the TIPc offers significant improvement in ride comfort.
- Add a load cell to the tow hook. The test driver noticed a difference in the longitudinal force feedback experienced by the towing vehicle, for the different trailer tyre pressures.
- Expand the TIPc scope to take into consideration safety, environmental, ride comfort and handling performance.
- Implement the TIPc on a passenger vehicle.
- Combine a pressure controlled tyre, smart suspension and smart anti-roll bar to improve high speed ride comfort and handling for vehicle, with a high centre of mass traveling on-road and off-road.

© University of Pretoria

This page is intentionally left blank

© University of Pretoria

7 References

Abdelghaffar, A., Hendy, A., Desouky, O. & Badr, Y., 2014. *Effects of Different Tire Pressures on Vibrational Transmissibility in Cars.* Prague, Czech Republic, International Conference on Mechanical Engineering and Mechatronics.

Adams, B. T., Reid, J. F., Hummel, J. W. & Zhang, Q., 2004. Effects of central tire inflation systems. *Journal of Terramechanics*, p. 5.

Becker, C. M., 2008. *Profiling of rough terrain.* Pretoria: Department of Mechanical and Aeronautical Engineering Faculty of Engineering, Built Environment and Information Technology.

Beckwith, T. G., Marangoni, R. G. & Lienhard V, J. H., 2007. *Mechanical Measurements.* 6 ed. Boston(Massachusetts): by Pearson Leaming Solutions.

Besselink, I. J. M., Schmeitz, A. J. C. & Pacejka, H. B., 2009. *An improved Magic Formula/Swift tyre model that can handle inflation pressure changes.* Stockholm, Vehicle System Dynamics : International Journal of Vehicle Mechanics and Mobility, pp. 337-352.

Bosch, H.-R., 2016. *FTire model parameterization and validation of an all-terrain SUV tyre.* Pretoria: Department of Mechanical and Aeronautical Engineering, University of Pretoria.

British Standards Institution 6841, 1987. *British Standard Guide to measurement and evaluation of human exposure to whole body mechanical vibration and repeated shock,* BS 6841: British Standards Institution.

Brondex, J., 2014. *Design of a prototype of an adaptive tire pressure system.* Stockholm: Department of Aeronautical and Vehicle Engineering Engineering.

Caban, J., Drozdziel, P., Barta, D. & Liscak, S., 2014. VEHICLE TIRE PRESSURE MONITORING SYSTEMS. *DIAGNOSTYKA*, 15(3).

Cao, P., Zhou, C., Jin, F. & Fan, X., 2016. Tire–Pavement Contact Stress with 3D Finite-Element Model: Part 1: Semi-Steel Radial Tires on Light Vehicles. *Journal of Testing and Evaluation.*

© University of Pretoria

Chegg, I., 2019. *Chegg Study*. [Online]
Available at: https://www.chegg.com/homework-help/definitions/normal-curve-31
[Accessed 12 September 2019].

CODA DEVELOPMENT, 2013. *SIT*. [Online]
Available at: http://www.selfinflatingtire.com/
[Accessed 02 October 2019].

Cosin scientific software, 2020. *cosin scientific software.* [Online]
Available at: https://www.cosin.eu/
[Accessed 17 February 2020].

Do Minh, C., Sihong, Z. & Yue , Z., 2013. Effects of tyre inflation and forward speed on vibration of an unsuspended tractor. *Journal of Terramechanics*, p. 2.

Els, P. S., 2005. The applicability of ride comfort standards to off-road vehicles. *Journal of Terramechanics*, Volume 42, pp. 47-67.

Els, P. S., 2006. *THE RIDE COMFORT VS. HANDLING COMPROMISE FOR OFF-ROAD VEHICLES.* Pretoria: FACULTY OF ENGINEERING, THE BUILT ENVIRONMENT AND INFORMATION TECHNOLOGY (EBIT) UNIVERSITY OF PRETORIA.

Els, P. S., Theron, N. J., Uys, P. E. & Thoresson, M. J., 2006. *The Ride Comfort vs. Handling Compromise for Off-Road Vehicles*, Pretoria: Mechanical and Aeronautical Engineering, University of Pretoria.

Eriksson, J. & Svensson, L., 2015. *Turning for Ride Quality in Autonomous Vehicle*, Uppsala: Uppsala Universitet.

Farroni, F. & Timpone, F., 2016. A Test Rig for Tyre Envelope Model Characterization. *Engineering Letters*, 24(3), pp. 45-49.

Fu, R.-S., 2015. *Polytropic Processes.* s.l.:s.n.

Gerotek, 2020. *GPS: S25"45.515 E028"00.522.* [Online]
Available at: https://www.armscor.co.za/?page_id=3967
[Accessed 13 February 2020].

© University of Pretoria

Gillespie, T. D. & Sayers, M., n.d. Role of Road Roughness in Vehicle Ride. *TransportatÍon Research Record.*

Gipser, M., n.d. *FTire, a New Fast Tire Model for Ride Comfort Simulations,* Germany: Esslingen University of Applied Sciences.

International Organization for Standardization 8608, 1995. *International Organization for Standardization ISO 8606: Mechanical vibration - Road surface profiles - Reporting of measured data,* s.l.: International Organization for Standardization.

Jinhwan, L., 2013. *Choked flow (Critical Flow).* s.l.:s.n.

Khanse, K. R., 2015. *Development and Validation of a Tool for In-Plane Antilock Braking System (ABS) Simulations.* Blacksburg(VA): Virginia Polytechnic Institute and State University.

Kirkby, N. F., 2011. *Polytropic Process.* [Online]
Available at: http://www.thermopedia.com/content/1045/
[Accessed 22 February 2018].

Kubba, A. E. & Jiang, K., 2014. A Comprehensive Study on Technologies of Tyre Monitoring Systems and Possible Energy Solutions. *sensors.*

McDonald, K. T., 2008. *Thermodynamics of a Tire Pump.* Princeton(New Jersey): Joseph Henry Laboratories Princeton University.

Mouleeswaran, S., 2012. Design and Development of PID Controller-Based Aactive Suspension System for Automobiles. In: *PID Controller Design Approaches - Theory, Tuning and Application to Frontier Areas.* Coimbatore: Springer.

MUNSON, B. R., YOUNG, D. F., OKIISHI, T. H. & HUEBSCH, W. W., 2009. *Fundamentals of Fluid Mechanics.* 6 ed. Hoboken(New Jersey): John Wiley & Sons.

Park, S. J. & Subramaniyam, M., 2013. Evaluating Methods of Vibration Exposure and Ride Comfort in Car. *Journal of the Ergonomics Society of Korea,* August, 32(4), pp. 381-387.

Petersen, W., 2009. *Volumetric off-road tire model for electric vehicle application.* s.l.:University of Waterloo Faculty of Engineering Department of Systems Design Engineering.

© University of Pretoria

Quick, D., 2012. *NEW ATLAS.* [Online]
Available at: https://newatlas.com/goodyear-air-maintenance-technology-tires/24229/
[Accessed 10 12 2019].

Sayers, M. & Karamihas, S. M., 1998. *The Little Book of Profiling.* s.l.:University of Michican.

Sherwin, L. M., Owende, P. M. O., Kanali, C. I. & Lyons, J., 2004. Influence of tyre inflation pressure on whole-body vibrations transmitted to the operator in a cut-to-length timber harvester. *Applied Ergonomics.*

Stallmann, M. J., 2014. *Tyre model verification over off-road terrain.* Pretoria: University of Pretoria.

Stallmann, M. J. & Els, P. S., 2014. Parameterization and modelling of large off-road tyres for rideanalyses: Part 2 – Parameterization and validation of tyre models. *Journal of Terramechanics,* pp. 85-94.

Taheri, S., Sandu, C., Taheri, S. & Pinto, E., 2015. a technical survey on Terramechanics models for tire-terrain interaction used in modeling and simulation of wheeled vehicles. *Journal of Terramechanics,* Volume 57, p. 17.

Uys, P. E., Els, P. S. & Thoresson, M., 2007. Suspension settings for optimal ride comfort of off-road vehicles travelling on roads with different roughness and speed. *Journal of Terramechanics,* 44(2), pp. 163-175.

Wang, S., 2013. *Multiple-Sensor Based Approach for Road Terrain Classification.* Sydney: Faculty of Engineering and Information Technology Centre for Autonomous Systems Intelligent Mechatronic Systems Group.

Ward, C. & Iagnemma, K., 2009. Speed-independent vibration-based terrain classification for passenger vehicles. *Vehicle System Dynamics,* September, 47(9), p. 1095–1113.

Wills, T., 2016. *What Tyre Pressure For Racing?.* [Online]
Available at: http://www.suspensionsetup.info/blog/what-tyre-pressure-for-racing-2
[Accessed 22 Oct 2017].

Zegelaar, P. W. A., 1998. *The dynamic response of tyres to brake torque variations and road unevenesses, PhD Thesis,* Delft, The Netherlands: Delft University of Technology.

© University of Pretoria

Žuraulis, V., van der Merwe, N., Scholtz, O. & Els, P. S., 2017. *MODELLING AND VALIDATION OF A TESTING TRAILER FOR ABS AND TYRE INTERACTION ON ROUGH TERRAIN*. Budapest, Hungary, Proceedings of the 19th International & 14th European-African Regional Conference of the ISTVS.

© University of Pretoria

This page is intentionally left blank

© University of Pretoria

© University of Pretoria